

Resurgence in the Virasoro Minimal String and 3d Gravity

Maximilian Schwick^a

^a*Albert Einstein Center for Fundamental Physics, Institute for Theoretical Physics,
University of Bern, CH-3012 Bern, Switzerland*

E-mail: maximilian.schwick@unibe.ch

ABSTRACT: We compute non-perturbative, resurgent contributions to the Virasoro minimal string and 3d gravity using techniques from hermitian matrix models. In particular, we construct a fully non-perturbative partition function for the Virasoro minimal string in terms of a Zak transform. In this context, negative tension D-branes appear naturally, which in the matrix model correspond to anti-eigenvalues, or instantons on the involuted sheet of the spectral curve. We further extend this analysis to resolvents and observe resurgent wall crossing phenomena between ZZ- and FZZT-branes. Using recent results that relate the Virasoro minimal string to 3d gravity with end-of-the-world branes we proceed to study the resurgent consequences of summing over the genus in 3d gravity, where we find non-perturbative contributions of doubly exponential type. These statements are then tested using resurgent large-order asymptotics. Lastly, we compute the non-perturbative eigenvalue density for generic hermitian matrix models and identify the change of asymptotic behavior at the edge of the eigenvalue distribution with a Stokes transition. This allows us to identify oscillations in the eigenvalue density with anti-Stokes behavior of FZZT-branes. In the case of 3d gravity with end-of-the-world branes we comment how this Stokes transition coincides with the onset of black hole behaviour and compute the non-perturbative primary density. Furthermore, we apply these techniques to the eigenvalue density of JT gravity to compute higher genus corrections.

KEYWORDS: Resurgence, Matrix Models, Virasoro Minimal String, Transseries, Resonance, Large-Order Resurgent Asymptotics, Stokes Data, Stokes Phenomena, 3d Gravity, Black Holes, JT Gravity, Wall Crossing, ZZ-Branes, FZZT-Branes, Negative Tension Branes, Nonperturbative Partition Functions

Contents

1	Introduction and Summary	2
2	Non-Perturbative Effects in the Virasoro Minimal String	4
2.1	Anti-Eigenvalues in the Virasoro Matrix Model	4
2.2	On Negative Branes from Boundary Conformal Field Theory	9
2.3	The JT Gravity Limit	11
2.4	Large-Order Resurgent Checks	12
2.5	Wall Crossing in the Virasoro Minimal String	14
3	Non-Perturbative Partition Function for the Virasoro Minimal String	17
3.1	Generic Non-Perturbative Completion of the Partition Function	17
3.2	Choosing a Non-Perturbative Completion	21
4	Non-Perturbative Effects in 3d Gravity	22
5	Black Hole Threshold as a Stokes Transition	26
5.1	Generic Construction	27
5.2	Example: The Virasoro Minimal String and 3d Gravity	32
5.3	Example: JT Gravity	36
A	Data for the Virasoro Minimal String	38

1 Introduction and Summary

Understanding non-perturbative contributions in string theory has been a fruitful area of study for many years. In this context the discovery of D-branes has opened many pathways [1, 2]. However explicit computations are hard to perform and therefore simple examples are of paramount importance. For this reason non-perturbative contributions in matrix models and minimal string theories have been studied extensively in recent years, e.g. [3–22]. In minimal string theory such contributions are due to ZZ- [23] and FZZT-branes [24, 25]. In the corresponding matrix model they are associated to eigenvalue tunnelling – the movement of eigenvalues in the diagonal matrix integral to non-perturbative saddles [6, 7].

Moreover, resurgent computations for the Painlevé I equation [26–28] as well as the Painlevé II equation [29, 30] – which compute the specific heat of (2,3) minimal (super-) string theory – suggested the existence of further non-perturbative contributions that are exponentially enhanced: Each falling instanton has an exponentially growing sibling, a phenomenon that is called resonance in the resurgence literature [11, 15]. Such contributions usually come with a minus sign in comparison to the standard instantons which suggests that in minimal string theory they correspond to branes with negative tension [18]. Using resurgent techniques [31] it was also argued that such instanton contributions appear in the asymptotics of generic string genus expansions [32, 18]. As it is central to this work we quickly review this argument in figure 1¹.

In parallel to the developments described above, the playground of minimal string theories has recently been extended by the construction of the Virasoro minimal string (VMS) [36]. It represents a continuous family of critical worldsheet theories indexed by $c \in \mathbb{R}_{\geq 25}$ and is given via

$$\left(\begin{array}{c} \text{Liouville CFT} \\ c \geq 25 \end{array} \right) \oplus \left(\begin{array}{c} \text{Liouville CFT} \\ \hat{c} = 26 - c \leq 1 \end{array} \right) \oplus \left(\begin{array}{c} \text{bc - ghosts} \\ -26 \end{array} \right). \quad (1.1)$$

For further details we refer the reader to the original paper [36]. Given the natural proximity of the VMS to other minimal string theories it is natural to ask if the non-perturbative contributions mentioned above find an analogue here: we use the methods developed in [6, 15, 18] to compute the exponential contributions to the free energy of the VMS. More specifically we will study the asymptotic behaviour of the free energy and the resolvent, where we find negative tension brane contributions in addition to resurgent wall crossing phenomena. In this context, we observe that not all falling non-perturbative exponentials in the VMS have their origins on the physical sheet of the spectral curve – some standard falling D-brane contributions in fact originate in the non-physical sheet.

Putting all the contributions together we can construct the full non-perturbative partition function for the VMS – meaning the full family of non-perturbative completions allowed by resurgence. This proposal is based on [37] and we generalize it to the VMS: In this way we can write the partition function as a sum over filling fractions in the spirit of [7, 38] and present checks on its validity by comparing to the previously computed non-perturbative effects. Consequently we discuss possible choices of non-perturbative completion – firstly a minimal choice consistent with median summation and secondly a generic choice showing quasi-periodic asymptotics.

It has been shown in [39, 40], that the VMS describes a sub-sector of 3d gravity: Specifically in [40] a map is constructed between the VMS and 3d gravity path integrals on manifolds that are topologically a thickened Riemann surface $\Sigma_{g,n} \times I$, where g counts the genus, n is the number of boundaries and I is an interval with end-of-the-world (EOW) branes on both ends. We use this

¹For reviews of 1-summability and resurgence the interested reader may consult [33–35].

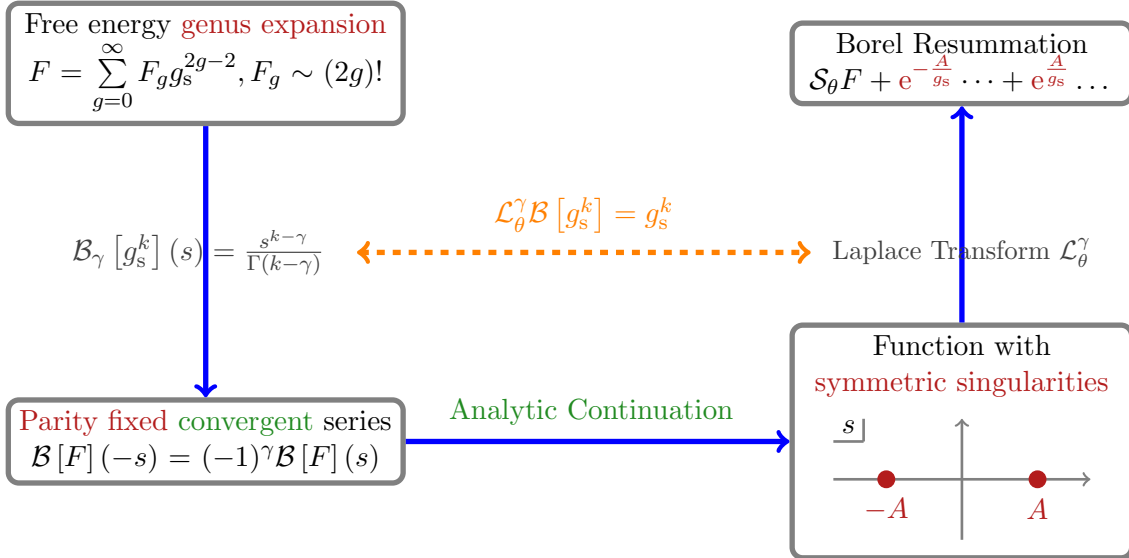


Figure 1: Pictorial description of the Borel resummation of a divergent series with genus expansion. Start with the left-downward arrow by performing a Borel transform \mathcal{B}_γ , which yields a power-series convergent in a disk around the origin ($\gamma \in \mathbb{R}$ see [33–35] for details). Moreover, because we started with a genus expansion the Borel transform and its analytic continuation will be parity fixed – the resulting Borel-plane singularities will be symmetrically arranged. The final step with the right-upward arrow is resummation via Laplace transform $\mathcal{L}_\theta^\gamma$ along the angle θ (inverse Borel transform); such transformation will turn the Borel plane singularities into exponential contributions where the location of the singularity determines the exponential weight. Therefore, because of the symmetry on the Borel plane that we inherited from the genus expansion, such exponentials appear always in pairs $(A, -A)$ – a phenomenon often referred to as *resonance*. Notice how this argument is independent of the choice of parameter γ . This figure illustrates and builds on a graphic from [15].

map to explore the resurgence non-perturbative effects that arise if one sums over the genus in 3d gravity. For our specific example we pick $n = 2$ and try to understand the effects of the genus sum by using the VMS non-perturbative predictions. We find doubly exponential contributions in c as expected in [39], which we further confirm with asymptotic checks. In addition we also find both positive and negative instantons, just as in the VMS. In this context it could be interesting to generalize the closed form VMS partition function from section 3 to correlators ($n > 0$).

Last but not least we compute the non-perturbative eigenvalue density for hermitian matrix models with resurgent methods. In this way we can understand the change of asymptotic behaviour that occurs at the edge of the eigenvalue distribution as a Stokes transition of FZZT-branes. Consequently we find a formula for the non-perturbative density that has a universal, oscillating piece – next to additional non-perturbative effects that depend on the choice of non-perturbative completion. This formula is a generalization of a proposal for the non-perturbative eigenvalue density in [10]. We then connect this discussion to 3d and JT gravity where the edge of the eigenvalue spectrum is identified with the onset of the Cardy growth of states and compute the associated non-perturbative densities.

This paper is organized as follows: in section 2 we will apply the matrix model formalism of [6, 15, 18] to the VMS and collect results. Here in subsection 2.1 we first focus on the physical sheet

instantons and compare with literature results. Thereafter we compute the previously mentioned, new, non-physical sheet contributions. In subsection 2.2 we reproduce negative tension brane contributions directly from boundary conformal field theory. Subsection 2.3 is dedicated to the Jackiw–Teitelboim two-dimensional dilaton gravity (JT) [41, 42] limit of the formulae produced in subsection 2.1. Subsequently, we will perform an asymptotic large-order study of the free energy in subsection 2.4 to numerically confirm our previous results. In this context it is natural to also perform large order checks on the corresponding resolvent, which yields wall crossing phenomena between ZZ- and FZZT-branes. This is the topic of section 2.5. Putting the above together, we can conjecture a fully non-perturbative partition function for the VMS in section 3 and check it against previously computed non-perturbative contributions. Here we will construct the generic transseries – meaning the full family of resurgent non-perturbative contributions – in subsection 3.1 and comment on specific non-perturbative completions in subsection 3.2. Having established the VMS non-perturbative effects we import them to a subsector of 3d gravity using the map established in [40] to find doubly exponential contributions. This is the content of section 4. Lastly, in section 5 we consider a generic hermitian matrix model and compute the non-perturbative density from resurgent contributions. In subsection 5.1 we present the generic construction for hermitian matrix models, and connect this discussion to 3d and JT gravity in subsections 5.2 and 5.3 respectively.

2 Non-Perturbative Effects in the Virasoro Minimal String

In this section we apply recent progress in the non-perturbative study of matrix models and their double scaling limits [6, 7, 15, 18, 43] to the VMS. More precisely, explicit formulae have been developed that allow the direct computation of exponential corrections (resurgent instantons) purely from special geometry². Here we apply those methods to the free energy of the VMS [36] to compute explicitly the non-perturbative effects. Let us stress that these methods come from hermitian matrix models: To make sure that they indeed apply to the VMS³ we perform explicit numerical large order checks⁴. By doing so we will predict and numerically verify contributions from negative tension branes – additional effects that were initially not observed in [36]. Lastly we will study the VMS resolvent and verify the existence of wall crossing phenomena between ZZ- and FZZT-branes. In the following we will adhere exactly to the conventions of [36].

2.1 Anti-Eigenvalues in the Virasoro Matrix Model

We are interested in non-perturbative corrections to the free energy [36]

$$F_V \simeq \sum_{g=0}^{\infty} F_{V,g} g_s^{2g-2}, \quad (2.1)$$

where we use the subscript V to indicate that we are specialising to the VMS. This is an asymptotic series of factorial growth $F_{V,g} \sim (2g)!$ which already suggests the existence of exponential

²Meaning that the ingredients needed to employ these formulae are: the spectral curve with a differential on it, and the Bergman kernel [44].

³This is non-trivial in the sense that the VMS does not have an explicit hermitian matrix model underlying it – it just fulfils topological recursion, which is a more generic framework.

⁴This will be important for section 3 where we make a conjecture for the non-perturbative partition function of the VMS based on matrix model arguments.

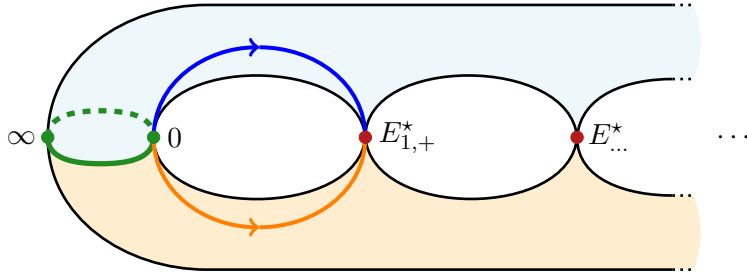


Figure 2: The spectral curve of the VMS. We show the branch cut (green) starting at 0 and ending at ∞ . Furthermore we visualize the two sheets: the physical sheet on top (light blue) and the non-physical sheet at the bottom (light orange). Those two sheets meet at the cut and at the saddle points (2.7) (red). In addition we show the integration cycle (blue) of the suppressed instanton action (2.6) associated to the saddle point $E_{1,+}^*$ in the physical sheet. On the other hand, for the same saddle-point $E_{1,+}^*$, we also show the integration cycle (orange) associated to the exponentially growing instanton (2.15) on the non-physical sheet. Both contributions are seen by the asymptotics of the free energy (see section 2.4). This plot builds on previous graphics from [15, 18].

corrections. The explicit coefficients $F_{V,g}$ can be computed by running the topological recursion [44] on the associated spectral curve. For an energy E it is given by⁵

$$y_V(E) = -2\sqrt{2\pi} \frac{\sin(2\pi b\sqrt{-E}) \sin(2\pi b^{-1}\sqrt{-E})}{\sqrt{-E}}, \quad (2.2)$$

with the standard matrix model differential and Bergman kernel [36]. Furthermore we have the usual relation $c = 1 + 6(b + b^{-1})^2$. This spectral curve has a square-root branch cut starting at the branch point $a = 0$ and ending at positive infinity. This is shown in figure 2. See appendix A for some explicit free energy coefficients.

Physical Sheet Instanton Corrections: We start by computing the well-known instanton corrections to the free energy (2.1) of the form

$$\mathcal{F}^{(n)} \simeq e^{-n \frac{A}{g_s}} \text{ (asymptotic series in } g_s \text{)}, \quad (2.3)$$

by using the formulae developed in [6, 11, 18]. Here non-perturbative contributions to the free energy of generic one-cut matrix models are computed through eigenvalue tunnelling, where n counts the number of eigenvalues that have tunneled to a non-perturbative saddle. Those formulae can be adapted to hold for the double scaling limit as well by moving one of the endpoints of the spectral curve to infinity [11, 18]. Let us quickly state the result for a general double scaled configuration and then specialize to the VMS: focus on a saddle-point E^* of a generic double scaled curve of the form

$$y(E) = M(E)\sqrt{-E}, \quad (2.4)$$

with one cut running from the branch point $a = 0$ to positive infinity. Here we require the moment function $M(E)$ to be analytic at the origin. Then the lowest contributing g_s order to

⁵We follow exactly the conventions of [36].

the one instanton is given by⁶ [11, 18]

$$\mathcal{F}^{(1)} \simeq e^{-\frac{A}{g_s}} \left(\frac{1}{4} \sqrt{\frac{g_s}{4\pi M'(E^*)(a - E^*)^{\frac{5}{2}}}} + O(g_s^{3/2}) \right), \quad (2.5)$$

with the instanton action given by

$$A = 2 \int_a^{E^*} y(E) dE, \quad (2.6)$$

where we have chosen the integration path in the principle sheet of y (see the blue integration contour in figure 2). Notice also the factor of 2 that promotes the half cycle in (2.6) to a full cycle. Specialising the above to the VMS we find, for each saddle point

$$E_{k,\pm}^* = -\frac{k^2 b^{\pm 2}}{4}, \quad k \in \mathbb{Z}_{\geq 1}, \quad (2.7)$$

the corresponding free energy contribution and their instanton action

$$\mathcal{F}_{V,k,\pm}^{(1)} \simeq \frac{\sqrt{(-1)^k g_s}}{4 \cdot 2^{3/4} \pi^{3/2} \sqrt{b^{\pm 1} \sin(b^{\pm 2} \pi)}} e^{-\frac{A_{k,\pm}}{g_s}} + \dots, \quad A_{k,\pm} = \frac{4\sqrt{2} b^{\pm 1} (-1)^{k+1} \sin(\pi k b^{\pm 2})}{1 - b^{\pm 4}}. \quad (2.8)$$

This result indeed agrees with the one presented in [36]. For the asymptotic tests in section 2.4 we will need the instanton contribution with the smallest action ($k = 1, +$). We have

$$\mathcal{F}_{V,1,+}^{(1)} \simeq \frac{i\sqrt{g_s}}{4 \cdot 2^{3/4} \pi^{3/2} \sqrt{b \sin(b^2 \pi)}} e^{-\frac{1}{g_s} \frac{4\sqrt{2} b \sin(b^2 \pi)}{1 - b^2}} + \dots. \quad (2.9)$$

Having established the one-instanton correction it is natural to compute higher instanton contributions. The formula is most conveniently written as a ratio of partition functions and reads for a generic double scaled curve [18]

$$\frac{\mathcal{Z}^{(\ell)}(g_s)}{\mathcal{Z}^{(0)}(g_s)} \simeq \frac{G_2(\ell + 1)}{(2\pi)^{\ell/2}} e^{-\frac{\ell}{g_s} (V_{h,\text{eff}}(E^*) - V_{h,\text{eff}}(a))} \left(\frac{g_s}{32M'(E^*)(a - E^*)^{5/2}} \right)^{\frac{\ell^2}{2}} + \dots. \quad (2.10)$$

This result means that to each saddle point we are led to associate an infinite tower of instantons – integer multiples of the same action. In the matrix model such contributions are created by tunnelling multiple eigenvalues to the same saddle. Notice furthermore that the starting genus is quadratic in the instanton number ℓ which is consistent with previous results [7]. Specializing the above formula to the VMS we arrive at the multi-instanton prediction

$$\frac{\mathcal{Z}_{V,k,\pm}^{(\ell)}(g_s)}{\mathcal{Z}_V^{(0)}(g_s)} \simeq 2^{-\frac{1}{4}\ell(2+9\ell)} \pi^{-\frac{1}{2}\ell(1+2\ell)} G_2(1 + \ell) e^{-\ell \frac{4\sqrt{2} b^{\pm 1} (-1)^{k+1} \sin(\pi k b^{\pm 2})}{g_s(1 - b^{\pm 4})}} \left(\frac{g_s (-1)^k}{k^2 b^{\pm 1} \sin(k\pi b^{\pm 2})} \right)^{\frac{\ell^2}{2}} + \dots \quad (2.11)$$

⁶Notice the minus sign in comparison to [18]. This is because in [18] the cut was assumed to run to negative infinity instead of positive infinity. The additional factor of 2 in comparison to [18] in front of the integral (2.6) and in front of the moment function is due to the fact that we have only considered a half cycle [18].

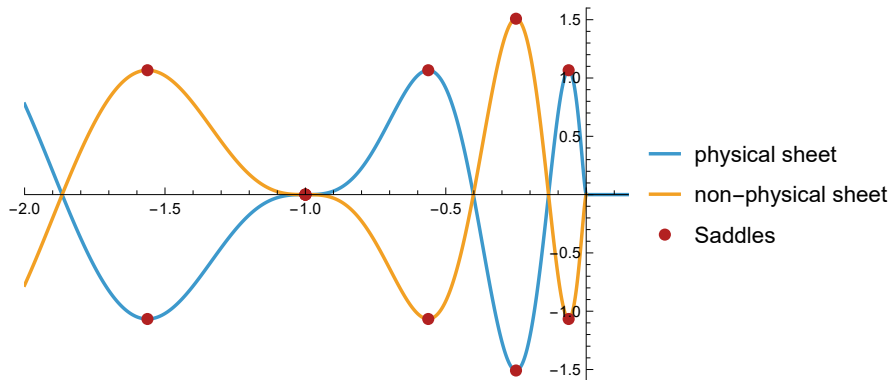


Figure 3: Depiction of the effective potential $V_{\text{eff}}(E) = \int dEy(E)$ as a function of E at $b = 1/2$. Same as the spectral curve (2.2) it has two sheets: the physical sheet (light blue) and the non-physical one (light orange). Compare also to figure 2. The saddles (red) of the potential on the physical sheet are exactly the resurgent instanton actions (2.6) and we can indeed see that they oscillate between positive and negative values. In addition, taking into account the non-physical sheet we find additional saddle points (red) (On the uniformization cover each saddle point splits into two, see for example formula (2.15).), exactly with a relative minus sign in comparison with the physical sheet.

Having computed those non-perturbative contributions we observe a peculiar fact. The instanton actions (2.6) are not all positive (see also (2.8)) – we do not only find falling exponentials from the physical sheet of the spectral curve. This is consistent with findings in minimal string theory [11, 18]. See figure 3 for an illustration. This issue is exactly resolved through the discussion in [15, 18] that stipulates that one should also take into account contributions from the non-physical sheet. Indeed this gives additional resurgent instanton actions exactly with a relative minus sign – the missing falling exponentials (see again figure 3). In fact, this means indeed that all instantons appear in resonant pairs (a falling and a growing exponential) – exactly as expected from a string genus expansion (see also figure 1)⁷ [18].

Instantons from the Non-Physical Sheet: After having computed known non-perturbative corrections, we now turn to uncover new resurgent contributions: as mentioned already in the introduction, the VMS is *resonant*, meaning for each resurgent instanton action A it will have a sibling instanton action $-A$ [15]. This can be seen at the level of a generic spectral curve of the form (2.4) as follows: the curve, as a function of E , has square-root double-sheeted structure. We introduce the uniformizing coordinate $z^2 = -E$ with the involution map σ given by⁸

$$z \rightarrow \sigma(z) = -z, \quad (2.12)$$

such that

$$E(\sigma(z)) = E(z), \quad \mathcal{Y}(\sigma(z)) = -\mathcal{Y}(z), \quad (2.13)$$

where on the principal sheet we have identified $\mathcal{Y}(z) = y(E(z))$ – meaning $\mathcal{Y}(z)$ is the spectral curve in uniformized variables. Notice that in the uniformization formulation each saddle-point

⁷At this point one might wonder whether the original nomenclature of physical and non-physical sheet still makes sense for the VMS – as there are falling (meaning physical) exponentials also on the non-physical sheet.

⁸Details on the subsequent discussion can be found in [15].

E^* now splits into two saddles that we will denote by

$$z^*, \quad \bar{z}^* = -z^*. \quad (2.14)$$

Also, in our nomenclature we follow [15] and by $\bar{\bullet}$ we mean the non-physical sheet and not complex conjugation. With the above terminology we are ready to reformulate our computation of the resurgent instanton action, but this time taking all sheets into account. On the principle sheet we still have exactly formula (2.6) but on the involuted sheet we find [15]

$$\bar{A} = 2 \int_0^{\bar{z}^*} dz \frac{\partial E}{\partial z} \mathcal{Y}(z) = 2 \int_0^{z^*} dz \frac{\partial E}{\partial z} \mathcal{Y}(\sigma(z)) = -2 \int_0^{z^*} dz \frac{\partial E}{\partial z} \mathcal{Y}(z) \equiv -A. \quad (2.15)$$

This means that for each saddle-point E^* we should not expect to find just one instanton action but two – one for each sheet. The integration contours on the spectral curve are explicitly visualized in figure 2. For this reason it is common to introduce the notation

$$\mathcal{F}^{(n|m)} \simeq e^{-(n-m)\frac{A}{g_s}} \text{(asymptotic series in } g_s), \quad (2.16)$$

where n, m label multiples of the exponential contributions associated to the uniformized saddles z^*, \bar{z}^* respectively. Such contributions have been computed extensively in [15, 18] and we want to apply the formulae derived therein to the VMS. The simplest such contribution is that of a single involuted sheet instanton, which for the generic curve (2.4) reads [18]

$$\begin{aligned} \mathcal{F}^{(0|1)} &\simeq e^{\frac{A}{g_s}} \frac{1}{4} \sqrt{\frac{g_s}{-4\pi M'(E^*)(a - E^*)^{\frac{5}{2}}}} + \dots = \\ &\simeq -ie^{\frac{A}{g_s}} \frac{1}{4} \sqrt{\frac{g_s}{4\pi M'(E^*)(a - E^*)^{\frac{5}{2}}}} + \dots, \end{aligned} \quad (2.17)$$

where the correct sign choice in the second equality was determined in [18]. For the VMS this contribution then reads

$$\mathcal{F}_{V,k,\pm}^{(0|1)} \simeq \frac{-i\sqrt{(-1)^k g_s}}{4 \cdot 2^{3/4} \pi^{3/2} \sqrt{b^{\pm 1} \sin(b^{\pm 2} \pi)}} e^{\frac{1}{g_s} \frac{4\sqrt{2}b^{\pm 1} (-1)^{k+1} \sin(\pi k b^{\pm 2})}{1-b^{\pm 4}}} + \dots. \quad (2.18)$$

Let us comment on this expression: it is very close to its resonant sibling (2.8) – the only difference being a global phase and the sign in the exponential. Though small, these differences are crucial for the asymptotic analysis which will be explored in detail in section 2.4. Furthermore, one might worry about the sign in the exponential contribution and the physical instabilities that it might carry: here it is important that in this work we never consider such contributions on their own but solely as non-perturbative corrections to the free energy – which we can control using resurgence methods⁹.

Having established the simplest resonant instanton let us turn to a rather non-trivial contribution: the (1|1) sector. From [45] one might get the impression that the annulus diagram between a brane and a negative tension brane should be trivial but that turns out not to be the

⁹In fact we will see in section 3 how such growing instanton effects can contribute to a Zak transform formulation of the partition function. See also [37].

case: indeed this contribution does not come with exponentials attached, but one still finds a non-trivial asymptotic series. The generic prediction for its lowest order reads [15, 18]

$$\mathcal{F}^{(1|1)} \simeq \frac{i}{2\pi g_s} A + O(g_s), \quad (2.19)$$

meaning for the VMS at the saddle point $E_{k,\pm}^*$ we find

$$\mathcal{F}_{V,k,\pm}^{(1|1)} \simeq \frac{i}{2\pi g_s} \frac{4\sqrt{2}b^{\pm 1}(-1)^{k+1} \sin(\pi k b^{\pm 2})}{1 - b^{\pm 4}} + O(g_s). \quad (2.20)$$

As a last non-trivial resonant computation we want to present a result for the (2|1) contribution. For details on this contribution we refer the reader to [15, 18] and we will here merely present the result. For an arbitrary curve of the form (2.4) it is most conveniently written as

$$\begin{aligned} \frac{\mathcal{Z}^{(2|1)}(g_s)}{\mathcal{Z}^{(0|0)}(g_s)} - \frac{\mathcal{Z}^{(1|0)}(g_s)}{\mathcal{Z}^{(0|0)}(g_s)} \frac{\mathcal{Z}^{(1|1)}(g_s)}{\mathcal{Z}^{(0|0)}(g_s)} &\simeq e^{-\frac{1}{g_s}(V_{h,\text{eff}}(E^*) - V_{h,\text{eff}}(a))} \times \\ &\times \frac{i}{8(2\pi)^2} \sqrt{\frac{2\pi g_s}{M'(E^*)(a - E^*)^{5/2}}} \left\{ 2\gamma_E + \log\left(\frac{2^8}{g_s^2} M'(E^*)^2 (a - E^*)^5\right) \right\} + \dots \end{aligned} \quad (2.21)$$

Plugging in the VMS spectral curve we arrive at

$$\begin{aligned} \frac{\mathcal{Z}_{V,k,\pm}^{(2|1)}(g_s)}{\mathcal{Z}_V^{(0|0)}(g_s)} - \frac{\mathcal{Z}_{V,k,\pm}^{(1|0)}(g_s)}{\mathcal{Z}_V^{(0|0)}(g_s)} \frac{\mathcal{Z}_{V,k,\pm}^{(1|1)}(g_s)}{\mathcal{Z}_V^{(0|0)}(g_s)} &\simeq e^{-\frac{1}{g_s} \frac{4\sqrt{2}b^{\pm 1}(-1)^{k+1} \sin(\pi k b^{\pm 2})}{1 - b^{\pm 4}}} \times \\ &\times \frac{i}{16 \cdot 2^{3/4} \pi^{5/2} k} \sqrt{\frac{g_s (-1)^k}{b^{\pm 1} \sin(\pi b^{\pm 2} k)}} \left\{ 2\gamma_E + \log(2^9 b^{\pm 2} k^4 \pi^4 \sin(b^{\pm 2} k \pi)) \right\} + \dots \end{aligned} \quad (2.22)$$

To finish this section let us further comment that the above contributions can be conveniently assembled into a (schematic) transseries structure. Including the contributions from just one singularity it is of the form

$$F \simeq \sum_{n,m} \sigma_1^n \sigma_2^m F^{(n|m)}(g_s). \quad (2.23)$$

We can generalize this to multiple – say κ – saddles where we arrive at

$$F \simeq \sum_{n,m \in \mathbb{N}^\kappa} \prod_{i=1}^{\kappa} \sigma_{i,1}^{n_i} \sigma_{i,2}^{m_i} F^{(n_1|m_1), \dots, (n_\kappa|m_\kappa)}(g_s), \quad (2.24)$$

which for the partition function $Z = \exp(F)$ reads analogously. Notice that in all our above computations the transseries parameters σ_i have been set to specific Stokes constants which is also why we have changed notation from curly to straight letters when writing the transseries (2.24). Details on this can be found in [26, 15, 18] and we will elaborate on it further in the context of the partition function in section 3.

2.2 On Negative Branes from Boundary Conformal Field Theory

Having computed negative brane contributions using the matrix integral formalism in section 2.1 we comment briefly on the analogous result from asymptotic boundaries. It was shown in [36]

that the full double-sheeted spectral curve for the double-scaled Virasoro matrix integral can be obtained from the disk partition function by inverse Laplace transform

$$y_V(E) = \int_{-i\infty+\gamma}^{i\infty+\gamma} \frac{d\beta}{2\pi i} e^{\beta E} Z_{\text{disk}}^{(b)}(\beta), \quad (2.25)$$

where $\gamma \in \mathbb{R}_+$ such that we avoid the singularities of the disk partition function $Z_{\text{disk}}^{(b)}(\beta)$ to the right. Furthermore the parameter β can be interpreted as a boundary length. For further details we refer the reader to the original paper [36]. Formula (2.25) implies that also $Z_{\text{disk}}^{(b)}(\beta)$ "sees" both sheets of the spectral curve. It therefore suggests that one should be able to reproduce the negative tension brane contribution also from a direct ZZ-disk computation.

Let us quickly state the standard exponentiated ZZ-brane contribution. More specifically it was shown in [36] that the first exponential correction to the VMS free energy (2.8) can also be computed via

$$\mathcal{F}_{V,k,\pm}^{(1)} \simeq \exp \left(\text{Disk}^{(m,\pm)} + \text{Annulus}^{(m,\pm)} + \dots \right), \quad (2.26)$$

where the unmarked disk and the annulus are computed with standard ZZ-boundary conditions in the c theory and with "Half" ZZ-boundary conditions in the \hat{c} theory. Explicitly one considers the boundary state¹⁰

$$|\text{ZZ}_{(1,1)}^{(b)}\rangle \otimes |\widehat{\text{ZZ}}_{m,\pm}^{(ib)}\rangle. \quad (2.27)$$

One should furthermore mention that the ZZ-annulus at face value diverges due to an improper use of the Siegel gauge condition and it is therefore subject to a regularization using string field theory [13, 36]. Here one divergent boson and two divergent fermion modes in the annulus integral

$$\text{Annulus}^{(m,\pm)} = \int_0^\infty \frac{dt}{2t} \left(\sum_{\text{b}} e^{-2\pi h_{\text{b}} t} - \sum_{\text{f}} e^{-2\pi \hat{h}_{\text{f}} t} \right), \quad (2.28)$$

are cured via the assignment (for details we refer the reader to [13])

$$\int_0^\infty \frac{dt}{2t} (e^{2\pi t} + e^{-2\pi t} - 2) \longrightarrow -\frac{1}{2} \log \left(-2^5 \pi^3 \text{Disk}^{(m,\pm)} \right). \quad (2.29)$$

To compute negative tension contributions we are instructed to consider the ZZ-boundary state (2.27) with an overall minus sign¹¹. This will produce a minus sign in front of the disk contribution but leave the annulus untouched – up to the disk in the regularization prescription

¹⁰We again follow exactly the notations in [36].

¹¹The attentive reader might wonder that this overall minus sign is just a normalization issue, but this does not seem to be the case as the effects are clearly visible in the asymptotics of the free energy (see section 2.4).

(2.29). This minus will contribute as a global prefactor of $1/\sqrt{-1}$. Upon the appropriate choice of sign for the square-root we find

$$\mathcal{F}_{V,k,\pm}^{(0|1)} \simeq -i \exp \left(- \text{blue circle}^{(m,\pm)} + \text{blue annulus}^{(m,\pm)} + \dots \right), \quad (2.30)$$

This is exactly the familiar pre-factor of i between positive and negative tension instantons. Comparing with formula (2.18) yields perfect agreement¹².

2.3 The JT Gravity Limit

It was established in the original work [36] that in the limit $b \rightarrow 0$ ($c \rightarrow \infty$) the VMS reduces to JT-gravity upon scaling g_s by $(8\pi^2 b^2)^{3/2}$. Let us perform this map for the non-perturbative contributions computed above: This is a good check of our previous results because JT-gravity is known to be resonant – to have both positive and negative exponential corrections [11, 18, 43]. Furthermore we focus our study on the saddle-point closest to the origin ($k = 1, +$), as this is the one that has been checked numerically to great accuracy in the aforementioned publications. Let us start with the well-studied one-instanton contribution: we take formula (2.9) and take the JT gravity limit. We then find

$$\mathcal{F}_{V,1,+}^{(1)} \xrightarrow{\text{JT}} \mathcal{F}_{\text{JT},1}^{(1)} \simeq i \sqrt{\frac{g_s}{2\pi}} e^{-\frac{1}{g_s} \frac{1}{4\pi^2}} + \dots \quad (2.31)$$

This agrees exactly with the results in [18, 43]. Similarly we can proceed with the other non-perturbative contributions associated to higher instanton numbers

$$\frac{\mathcal{Z}_{V,1,+}^{(\ell)}}{\mathcal{Z}_V^{(0)}} \xrightarrow{\text{JT}} \frac{\mathcal{Z}_{\text{JT},1}^{(\ell)}}{\mathcal{Z}_{\text{JT}}^{(0)}} \simeq \frac{G_2(1+\ell)}{(2\pi)^{\ell/2}} (-g_s)^{\frac{\ell^2}{2}} e^{-\ell \frac{1}{g_s} \frac{1}{4\pi^2}} + \dots \quad (2.32)$$

We now come to the resonant contributions:

$$\mathcal{F}_{V,1,+}^{(0|1)} \xrightarrow{\text{JT}} \mathcal{F}_{\text{JT},1}^{(0|1)} \simeq \sqrt{\frac{g_s}{2\pi}} e^{\frac{1}{g_s} \frac{1}{4\pi^2}} + \dots, \quad (2.33)$$

$$\mathcal{F}_{V,1,+}^{(1|1)} \xrightarrow{\text{JT}} \mathcal{F}_{\text{JT},1}^{(1|1)} \simeq \frac{1}{g_s} \frac{i}{8\pi^3} + \dots \quad (2.34)$$

At this stage let us note that also for JT-gravity the (1|1) contribution is not trivial. This was already established in [18] by studying the JT limit of minimal string theory and our results agree with those presented therein. To finish this subsection let us also provide the JT limit of the (2|1) contribution

$$\begin{aligned} \frac{\mathcal{Z}_{V,1,+}^{(2|1)}(g_s)}{\mathcal{Z}_V^{(0|0)}(g_s)} - \frac{\mathcal{Z}_{V,1,+}^{(1|0)}(g_s)}{\mathcal{Z}_V^{(0|0)}(g_s)} \frac{\mathcal{Z}_{V,1,+}^{(1|1)}(g_s)}{\mathcal{Z}_V^{(0|0)}(g_s)} &\xrightarrow{\text{JT}} \frac{\mathcal{Z}_{\text{JT},1}^{(2|1)}(g_s)}{\mathcal{Z}_{\text{JT}}^{(0|0)}(g_s)} - \frac{\mathcal{Z}_{\text{JT},1}^{(1|0)}(g_s)}{\mathcal{Z}_{\text{JT}}^{(0|0)}(g_s)} \frac{\mathcal{Z}_{\text{JT},1}^{(1|1)}(g_s)}{\mathcal{Z}_{\text{JT}}^{(0|0)}(g_s)} \simeq \\ &\simeq \frac{1}{2\pi} \sqrt{\frac{g_s}{2\pi}} (\gamma_E - \log(g_s)) e^{-\frac{1}{g_s} \frac{1}{4\pi^2}} + \dots \end{aligned} \quad (2.35)$$

¹²One can furthermore try to reproduce the (1|1) contribution in formula (2.19) directly from conformal field theory. Such a computation has been performed in [18] by integrating over the FZZT moduli space to arrive at ZZ-brane computations. A direct computation of (2.19) from ZZ-branes along the lines of [13] would be very interesting.

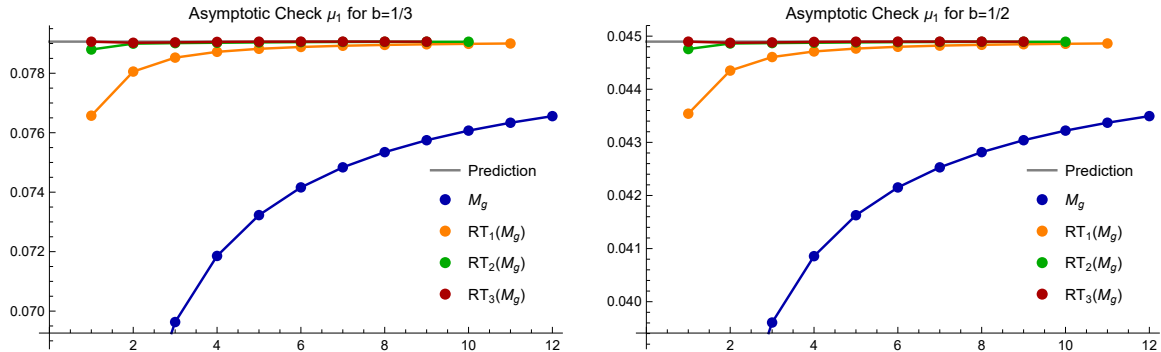


Figure 4: Plot of the sequence $M_g(b)$ and its Richardson transforms of order n RT_n as a function of g for the values $b = 1/3$ (left) and $b = 1/2$ (right). We also show the theoretical prediction in formula (2.43) in gray. Even though we do not have many terms in the asymptotic series we achieve an agreement of 5 digits with the predicted value.

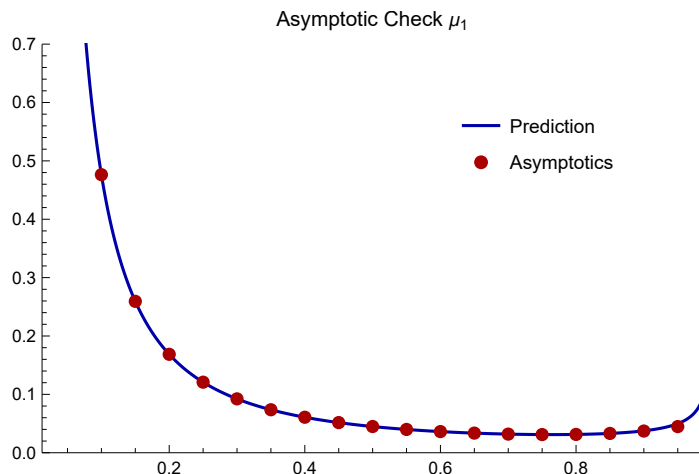


Figure 5: Plot of the numerical extrapolation $M_\infty(b)$ as a function of b . We also show the theoretical prediction in formula (2.43) in blue. The precision is 4 to 5 digits for each point, but seems to drop a little bit close to $b = 1$ exactly as expected in [36]. In fact a very similar plot has already appeared in [36]: The difference here is that here we got this plot from the corrected asymptotics (2.43) that take into account that the free energy is even.

2.4 Large-Order Resurgent Checks

Having established non-perturbative contributions to the free energy of the VMS we want to check if they are seen by large-order resurgent asymptotic methods. The slight difference between the analysis in [36] and the one performed here is the inclusion of negative tension branes which completely explains the asymptotics of the genus expansion of the free energy. To this end let us here recall quickly how the asymptotics of generic *even* asymptotic series are constructed [6, 26, 33]: consider a generic asymptotic perturbative series

$$\sum_{g \geq 0} a_g g_s^{g-2}. \quad (2.36)$$

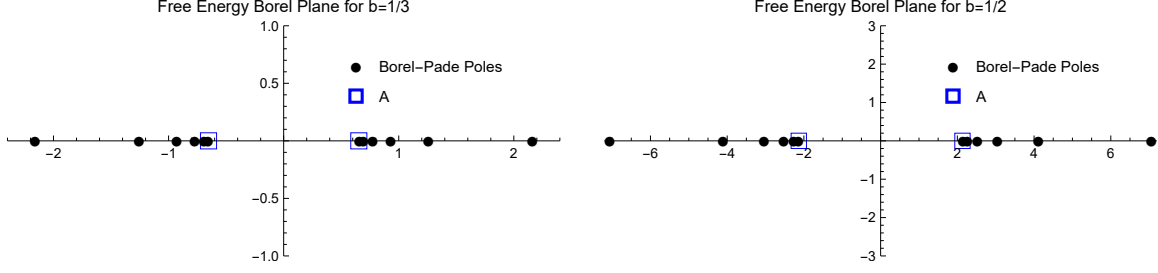


Figure 6: Plots of the poles of the Borel Padé approximant of the free energy for the VMS in the Borel plane. We have again chosen the values $b = 1/3$ (left) and $b = 1/2$ (right). We clearly see the resonance phenomenon where the instanton actions appear in pairs $(A, -A)$ – the Borel plane is indeed symmetric. Furthermore the locations of the Borel singularities agrees exactly with the prediction for those said actions.

For an exponential contribution of the form

$$ig_s^\beta e^{-\frac{A}{g_s}} \sum_{g \geq 0} c_g g_s^g, \quad (2.37)$$

the asymptotic contribution to the series (2.36) reads

$$a_k \sim \frac{1}{2\pi} \frac{\Gamma(k-2-\beta)}{A^{(k-2-\beta)}} \left(c_0 + c_1 \frac{A}{(k-2-\beta-1)} + \dots \right). \quad (2.38)$$

Notice how the perturbative series (2.36) in contrast to the free energy (2.1) also contains odd terms in g that equally appear in the asymptotic relation (2.38). This means that we are missing terms in the asymptotics that resolve this mismatch. This is exactly solved in our resonant setting: for each instanton action A we are instructed to also consider its resonant sibling $-A$, which contributes to the asymptotics as

$$a_k \sim \frac{1}{2\pi} \frac{\Gamma(k-2-\beta)}{(-A)^{(k-2-\beta)}} \left(\bar{c}_0 - \bar{c}_1 \frac{A}{(k-2-\beta-1)} + \dots \right). \quad (2.39)$$

Adding the two we find the total asymptotics

$$a_k \sim \frac{1}{2\pi} \frac{\Gamma(k-2-\beta)}{A^{(k-2-\beta)}} \begin{cases} \left(c_0 + \frac{\bar{c}_0}{(-1)^\beta} \right) + \left(c_1 - \frac{\bar{c}_1}{(-1)^\beta} \right) \frac{A}{(k-2-\beta-1)} + \dots, & k \text{ even,} \\ \left(c_0 - \frac{\bar{c}_0}{(-1)^\beta} \right) + \left(c_1 + \frac{\bar{c}_1}{(-1)^\beta} \right) \frac{A}{(k-2-\beta-1)} + \dots, & k \text{ odd,} \end{cases} \quad (2.40)$$

where cancellation of the odd contributions implies

$$c_0 - \frac{\bar{c}_0}{(-1)^\beta} = 0, \quad c_1 + \frac{\bar{c}_1}{(-1)^\beta} = 0, \quad \dots \quad (2.41)$$

Notice how this is exactly consistent with the sign changes in our previous formulae between brane (2.9) and negative brane contributions (2.17)¹³.

¹³This is where our asymptotic analysis differs from [36]: We take into account the fact that the perturbative series is even, which is why we find additional contributions.

Having reviewed the generic asymptotic formula for resonant problems let us apply it to the VMS. Here we focus on the instanton action

$$E_{1,+}^* = -b^2/4, \quad 0 < b < 1, \quad (2.42)$$

which is closest to the origin. Using formula (2.9) and (2.17) we find the leading large-order prediction

$$M_g(b) := \pi \frac{F_{V,g} A^{2g-\frac{5}{2}}}{\Gamma(k-\frac{5}{2})} \xrightarrow{g \rightarrow \infty} \frac{1}{4 \cdot 2^{3/4} \pi^{3/2} \sqrt{b \sin(b^2 \pi)}}, \quad (2.43)$$

where we remember

$$A = \frac{4\sqrt{2}b \sin(b^2 \pi)}{1 - b^2} \quad (2.44)$$

from formula (2.9). Let us now check the behavior of the auxiliary sequence $M_g(b)$ numerically. To this end we have produced explicitly the coefficients of the VMS free energy up to order $g = 14$ using the methods provided in [36]. We plot the sequence $M_g(b)$ together for various values of b in figure 4. Indeed in this way we verify formula (2.43) to 5 digits. Furthermore we can also plot the numerically extrapolated values for $M_\infty(b)$ against their analytical prediction. To this end we have taken the value of the third Richardson transform. This is visualized in figure 5.

To finish the numerical exploration of the free energy let us give more evidence for the resonant behavior of the VMS in an other way: For this we show a numerical approximation of the Borel plane singularities that is done via Padé approximants. The locations of those singularities correspond exactly to instanton actions¹⁴. The result is displayed in figure 6. Indeed we can clearly see the resonant behavior of the Borel plane, that predicts the instanton actions with both signs.

2.5 Wall Crossing in the Virasoro Minimal String

Having studied the free energy it is natural to extend this discussion to correlation functions – the simplest example being the resolvent. We want to study

$$R_1(E) = \left\langle \text{Tr} \frac{1}{E - M} \right\rangle \simeq \sum_{g=0}^{\infty} g_s R_{g,1}(E), \quad (2.45)$$

where we again follow the notation and conventions from [36] and the coefficients $R_{g,1}(-z^2)$ can be computed from the VMS curve (2.2) using topological recursion¹⁵. Further in this subsection we will often use the uniformization variable z given by $E = -z^2$. In the resolvent yet again new non-perturbative contributions appear: because of the explicit dependence of the resolvent on z we expect FZZT-like¹⁶ non-perturbative effects to play a role [43]. They are expected to have the instanton action

$$\tilde{A}(E) = 2 \int_0^E y_V(E) dE = \quad (2.46)$$

¹⁴Notice that the poles of the Padé approximant are mimicking branch cuts, meaning that we have to identify the instanton actions with the locations where the pole accumulations start.

¹⁵See for example formula (5.16) in [36].

¹⁶In this paper when referring to FZZT branes in the VMS we mean the hermitian matrix model analogue with instanton action (2.46) – which is expected to be consistent with putting FZZT boundary conditions on the spacelike Liouville sector and ZZ boundary conditions on the timelike one in the VMS [36].

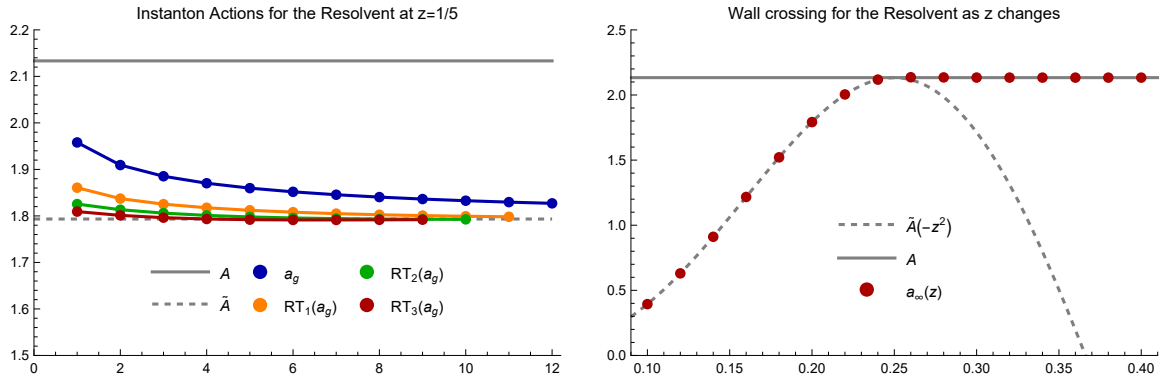


Figure 7: Visualization of the wall crossing phenomenon for the resolvent. On the left we check the appearance of the instanton action $\tilde{A}(-z^2)$ while on the right we visualize how it can disappear from the asymptotics as we vary z . On the left we plot the sequence a_g and its Richardson transforms of order n , namely RT_n , as a function of g . We show the theoretical prediction for the instanton action in formula (2.47) in gray for the case $z = 1/5 < 1/2$ and $b = 1/2$. Indeed the asymptotics follow the smaller instanton action $\tilde{A}(-z^2)$ in this case. On the right hand side we visualize the numerical extrapolation of a_∞ (y -axis) as we vary z (x axis) together with the theoretical prediction of the instanton actions. We still choose $b = 1/2$. Indeed we observe exactly the prediction (2.47) where the asymptotics sees the action $\tilde{A}(-z^2)$ until we reach $z = b/2$ and then the action A takes over.

$$= \frac{2\sqrt{2}b}{b^4 - 1} \left((1 + b^2) \sin \left[2\pi \left(b - \frac{1}{b} \right) \sqrt{-E} \right] + (1 - b^2) \sin \left[2\pi \left(b + \frac{1}{b} \right) \sqrt{-E} \right] \right),$$

which, in contrast to the ZZ instanton (2.44), is E dependent. Of those two actions ($\tilde{A}(E)$ for FZZT and A for ZZ contributions) the asymptotics will see the leading one – but only if it is turned on by resurgent relations. In other words it is natural to expect wall crossing phenomena to appear similarly to the minimal string discussion in [43]¹⁷. The natural expectation is that the wall (the crossing location) is located where the two actions agree: exactly at $z = \sqrt{-E_{1,+}^*} = b/2$ as in formula (2.42). For real z this translates to the following prediction for the asymptotics

$$a_g(z) := \sqrt{\frac{4g^2 R_{g,1}(-z^2)}{R_{g+1,1}(-z^2)}} \xrightarrow{g \rightarrow \infty} \begin{cases} \tilde{A}(-z^2), & z < \frac{b}{2}, \\ A, & z \geq \frac{b}{2}. \end{cases} \quad (2.47)$$

To check this let us first see that the instanton action (2.46) can really contribute to the asymptotics: fix the values $b = 1/2, z = 1/5$ which implies $\tilde{A} = 2/3 \cdot \sqrt{5} + \sqrt{5} < A = 32/15$. Then again using the terms up to $g = 14$ we can confirm the relation (2.47) with 3 digits after employing 3 Richardson transforms. The check is visualized on the left of figure 7.

Furthermore we can track the value of $a_{g \rightarrow \infty}$ as we vary z , using the approximation that we get from the third Richardson transform. This is shown on the right in figure 7. We clearly see how we first follow the action $\tilde{A}(-z^2)$ until we reach $z = b/2$ where A takes over.

Let us understand this wall crossing phenomenon further and give a detailed account of the whereabouts of the $\tilde{A}(-z^2)$ action for $z > b/2$: as shown in figure 7 clearly $\tilde{A}(-z^2) < A$ is still

¹⁷Notice that we are here referring to the resurgent wall crossing phenomenon, which just means that some Borel plane singularities switch sheet. This is a more general phenomenon than the well known discussion from supersymmetric gauge theories in [46].

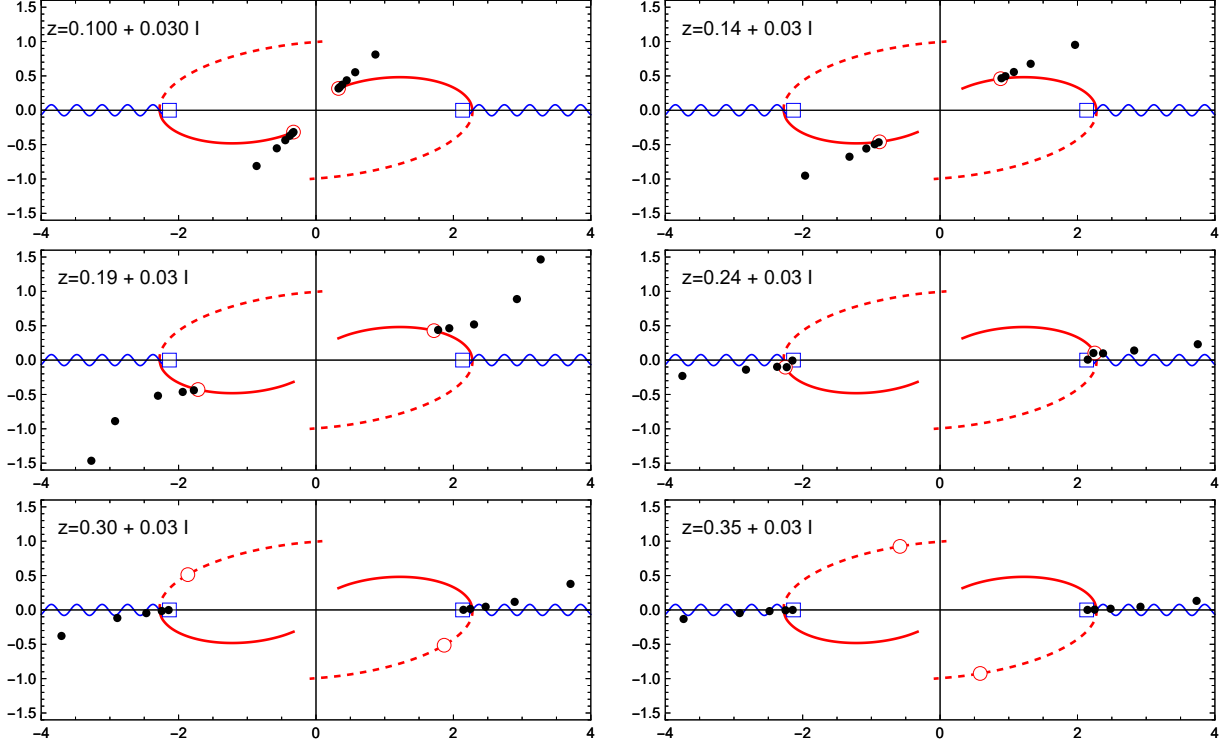


Figure 8: Visualization of the wall crossing phenomenon for the resolvent. We plot the Borel plane for the resolvent (2.45). The ZZ action A is shown as blue squares where the branch cut of the associated logarithmic singularity at A is visualized as a wiggly blue line. We want to study the movement of the singularity $\tilde{A}(-z^2)$ shown as a red path, where the small circles correspond to the value of $\tilde{A}(-z^2)$ for the various plots. Here we have taken z slightly above the real line to move from $1/10 + i\epsilon$ to $7/10 + i\epsilon$ and $b = 1/2$ (the plots are ordered from left to right, top to bottom). Each plot further shows in black the poles of the Borel-Padé approximant for the assigned value of z . Indeed we see how the singularity $\tilde{A}(-z^2)$ vanishes from the numerics as soon as it passes the branch cut of the stationary singularity A even though $|\tilde{A}| < |A|$. The underlying reason is that this singularity left the principle sheet of the Borel transformed resolvent. This is exactly the phenomenon of wall crossing. The presented plot builds on similar plots from [43].

true for $z > b/2$, yet the action no longer contributes to the asymptotics. The reason for this is that the Stokes constant associated to this action is turned off by a wall crossing phenomenon – this means that the action $\tilde{A}(-z^2)$ leaves the principle sheet of the Borel plane. This can be checked explicitly using Padé-approximants and the analysis is presented in figure 8: We vary the value of z on the real line with a slight imaginary offset such that the FZZT action (2.46) passes the branch cut created by the ZZ-brane (2.44). Then we visualize the Borel plane of the resolvent for various values of z along that path to check when the FZZT action is turned on or off. Indeed as shown in figure 8 once the FZZT action passes the branch cut, it leaves the principle sheet of the Borel plane and is no longer visible – it is turned off by a wall crossing phenomenon. We conclude that there are indeed FZZT like, non-perturbative contributions $\tilde{A}(-z^2)$ in the VMS, that are moreover subject to wall crossing phenomena. It is natural to expect that the same will hold for higher resolvents.

3 Non-Perturbative Partition Function for the Virasoro Minimal String

In this section we present a non-perturbative partition function for the VMS, meaning the complete resurgent family of non-perturbative completions indexed by 2 transseries parameters for each saddle point. The construction is based on [37] and is supported by our previous computations of non-perturbative VMS effects in section 2. We present the non-perturbative partition function in subsection 3.1. Finally we briefly discuss a sensible choice of non-perturbative completion in 3.2.

3.1 Generic Non-Perturbative Completion of the Partition Function

We can assemble the non-perturbative contributions computed above into a closed form transseries expression for the partition function given in terms of a Zak transform.

For this, let us first review a recent result for hermitian matrix models (HMM). Here, such a partition function was conjectured in [37]. We study a hermitian matrix model with a polynomial potential $V(\lambda)$ with $\kappa + 1$ saddles¹⁸ and N eigenvalues. Here we will be interested in the solution at large N , expanded around the one-cut configuration in the perturbative saddle with total 't Hooft parameter $t = g_s N$. The generic proposal comes from intuition in matrix integrals: Non-perturbative contributions are associated to eigenvalues that are tunnelling to other saddles of the spectral curve – where those eigenvalues accumulate and open new cuts [7]. The final result is the following, non-perturbative partition function for a hermitian matrix model^{19 20} [37]

$$Z^{\text{HMM}} \simeq \sum_{\ell \in \mathbb{Z}^\kappa} \prod_{i=1}^{\kappa} \rho_i^{\ell_i} \mathcal{Z}_G \left(\ell_i + \frac{\mu_i}{2\pi i} \right) \times \exp \left[\sum_{g=0}^{\infty} \hat{F}_g^{\text{HMM}} \left(t - g_s \left(\sum_{i=1}^{\kappa} \ell_i + \frac{\mu_i}{2\pi i} \right), g_s \left(\ell_1 + \frac{\mu_1}{2\pi i} \right), \dots, g_s \left(\ell_\kappa + \frac{\mu_\kappa}{2\pi i} \right) \right) g_s^{2g-2} \right], \quad (3.1)$$

where the gaussian partition function is computed as

$$Z_G(N) = \frac{g_s^{\frac{N^2}{2}}}{(2\pi)^{\frac{N}{2}}} G_2(1 + N), \quad (3.2)$$

and $\hat{F}_g^{\text{HMM}}(t_1, \dots, t_{\kappa+1})$ are the regularized multi-cut free energies of genus g , where each partial 't Hooft parameter t_i controls the size of the cut opened around the i -th saddle E_i^* . It is related to the standard multi-cut free energy $F_g^{\text{HMM}}(t_1, \dots, t_{\kappa+1})$ by subtracting the gaussian terms at each genus for each non-perturbative saddle [7, 47]

$$\hat{F}_g^{\text{HMM}}(t_1, \dots, t_{\kappa+1}) = F_g^{\text{HMM}}(t_1, \dots, t_{\kappa+1}) - \sum_{i=2}^{\kappa+1} \mathcal{F}_g^G(t_i), \quad (3.3)$$

where the asymptotic expansion of the gaussian reads

$$\mathcal{F}_0^G(t) = t^2 \left(\log(t) - \frac{3}{2} \right), \quad \mathcal{F}_1^G(t) = -\frac{1}{12} \log(t), \quad \mathcal{F}_g^G(t) = \frac{B_{2g}}{2g(2g-2)} t^{2-2g}, \quad g \geq 2. \quad (3.4)$$

¹⁸Meaning we have κ non-perturbative saddles and one perturbative one.

¹⁹Here the convention of μ_i has been chosen such that we have maximal symmetry between the backward and the forward transseries sectors. For details see [37].

²⁰It is interesting to compare the partition function (3.1) with a similar result in [38]. In fact (3.1) can be interpreted as the one cut limit of the result in [38].

Last but not least we have 2κ transseries parameters $\rho_i, \mu_i; i = 1, \dots, \kappa$, whose choice constitutes a non-perturbative completion of the partition function (see subsection 3.2). Notice also that this is an asymptotic series, which still needs to be resummed. For further details we refer the reader to [38, 37]. Let us also mention for completeness that there are 2 ways of computing the multi-cut free energy $F_g^{\text{HMM}}(t_1, \dots, t_{\kappa+1})$:

- It can be constructed directly from the original HMM potential via multi-cut spectral geometry and topological recursion – which, having the VMS in mind, is not useful as we do not have such an underlying potential²¹.
- It can be constructed as a series around the one-cut setting $\hat{F}_g^{\text{HMM}}(t, 0, \dots, 0)$ where each term can be computed from the original one-cut curve [7]. Notice that this type of series shows up naturally when expanding (3.1) in g_s . The simplest such example

$$\partial_{\nu_i} \hat{F}_g^{\text{HMM}} \left(t - \sum_{j=1}^{\kappa} \nu_j, \nu_1, \dots, \nu_{\kappa} \right) \Big|_{\nu_1=\dots=\nu_{\kappa}=0} = - \int_a^{E_i^*} y^{\text{HMM}}(E) dE \quad (3.5)$$

gives exactly the instanton action (2.6) up to a minus sign²² and the familiar factor of 2 that is due to the half-cycle integration in the matrix model as opposed to the full-cycle in the minimal string [18].

We now make the case that a similar construction as in [38, 37] also works for the VMS: The perturbative content of the VMS can be computed via topological recursion – a method born from hermitian matrix models. Moreover we have demonstrated in subsections 2.1, 2.4 and 2.5 above, how the non-perturbative contributions of the VMS can be computed with the non-perturbative hermitian matrix model formalism developed in [6, 7, 15, 18]. In fact we had emphasized how all the formulae we used are valid for generic one cut spectral curves. This suggests that the non-perturbative partition function for the VMS should be an analogue of (3.1), where the VMS version of the regularized multi-cut free energy can be computed as a series in terms of the VMS spectral curve as in (3.5). To write the explicit partition function for the VMS however we need to address the fact that the spectral curve (2.2) has infinitely many zeros: therefore let us momentarily assume that only κ saddles of the VMS are populated with eigenvalues²³. Furthermore the VMS spectral curve is of double scaled type (2.4). In the following we will write formulae based on the generic curve (2.4) but we keep in mind that we want to apply them to the VMS. We can then predict [37] the VMS partition function

$$Z_{\kappa}^V \simeq \sum_{\ell \in \mathbb{Z}^{\kappa}} \prod_{i=1}^{\kappa} \rho_i^{\ell_i} \mathcal{Z}_G \left(\ell_i + \frac{\mu_i}{2\pi i} \right) \exp \left[\sum_{g=0}^{\infty} f_g \left(g_s \left(\ell_1 + \frac{\mu_1}{2\pi i} \right), \dots, g_s \left(\ell_{\kappa} + \frac{\mu_{\kappa}}{2\pi i} \right) \right) g_s^{2g-2} \right], \quad (3.6)$$

where $f_g(\nu_1, \dots, \nu_{\kappa})$ is the double scaled analogue of the multi-cut free energy in formula (3.1). Furthermore each $f_g(\nu_1, \dots, \nu_{\kappa}) : \mathbb{C}^{\kappa} \rightarrow \mathbb{C}$ is analytic at the origin and we can give explicit

²¹A proposal for constructing a multi-cut curve underlying the double scaled analogue of F^{HMM} will be made in [48].

²²In comparison to the s variable commonly introduced in matrix models [7, 37] there is exactly a minus sign in comparison with the ν_i variable used here.

²³Later on we can still take κ to infinity to get the full result for the VMS. In practice considering only finitely many contributions for each computation suffices.

expressions for its derivatives in terms of the curve (2.4) (or (2.2) for the VMS). If no eigenvalues have tunneled it reduces to the perturbative free energy, which can be computed from topological recursion. In the case of the VMS we then find

$$f_g(0, \dots, 0) = F_{V,g}, \quad (3.7)$$

which was already discussed in (2.1). In the same spirit, its derivatives can be computed for any saddle E_i^* , $i = 1, \dots, \kappa$. The first few read [37]

$$\partial_{\nu_i} f_0(\nu_1, \dots, \nu_\kappa) \Big|_{\nu_1 = \dots = \nu_\kappa = 0} = -2 \int_a^{E_i^*} y(E) dE = - \oint_{B_i} y(E) dE, \quad (3.8)$$

$$\partial_{\nu_i}^2 f_0(\nu_1, \dots, \nu_\kappa) \Big|_{\nu_1 = \dots = \nu_\kappa = 0} = -\log \left(32 (a - E_i^*)^{5/2} M'(E_i^*) \right), \quad (3.9)$$

$$\begin{aligned} \partial_{\nu_i}^3 f_0(\nu_1, \dots, \nu_\kappa) \Big|_{\nu_1 = \dots = \nu_\kappa = 0} &= -\frac{8(a - E_i^*)^2 M''(E_i^*)^2 + 77M'(E_i^*)^2}{16(a - E_i^*)^{5/2} M'(E_i^*)^3} - \\ &+ \frac{2(a - E_i^*) M'''(E_i^*) + 17M''(E_i^*)}{4(a - E_i^*)^{3/2} M'(E_i^*)^2} + \frac{4}{(a - E_i^*)^{3/2} M(a)}, \end{aligned} \quad (3.10)$$

$$\begin{aligned} \partial_{\nu_i} f_1(\nu_1, \dots, \nu_\kappa) \Big|_{\nu_1 = \dots = \nu_\kappa = 0} &= -\frac{4(a - E_i^*)^2 M''(E_i^*)^2 + 19M'(E_i^*)^2}{192(a - E_i^*)^{5/2} M'(E_i^*)^3} + \\ &+ \frac{2(a - E_i^*) M'''(E_i^*) - M''(E_i^*)}{96(a - E_i^*)^{3/2} M'(E_i^*)^2} + \frac{M(a) - 3(a - E_i^*) M'(a)}{24(a - E_i^*)^{3/2} M(a)^2}, \end{aligned} \quad (3.11)$$

where in accordance with our generic curve (2.4) we have to set the endpoint of the cut $a = 0$. Notice also, that in contrast to the half cycles (3.5) in matrix models, in the double scaling limit people often express things in terms of full cycles on the spectral curve as in (3.8) [49, 50]. We are here following this convention and have therefore included all the appropriate factors of 2 regarding the full cycles of the double scaling limit in the expressions (3.8)-(3.11)²⁴. The more involved case with 2 saddles $E_i^*, E_j^*, i \neq j$ goes as follows[37]

$$\partial_{\nu_j} \partial_{\nu_i} f_0(\nu_1, \dots, \nu_\kappa) \Big|_{\nu_1 = \dots = \nu_\kappa = 0} = -4 \operatorname{arctanh} \left[\sqrt{\frac{a - E_i^*}{a - E_j^*}} \right], \quad (3.12)$$

where again $a = 0$. In principle the production of these derivative formulae is algorithmic following [7, 18], but computations quickly become very involved. Nevertheless the above expressions can be immediately applied to the VMS spectral curve (2.7) to compute the full non-perturbative partition function as an asymptotic series in g_s ²⁵. In addition it fully includes all non-perturbative ZZ-brane contributions in the VMS (See formulae (3.14), (3.15) and (3.16)). Having established the computation of $f_g(\nu_1, \dots, \nu_\kappa)$ let us study the non-perturbative proposal (3.6) in more detail: We have 2κ transseries parameters $\rho_i, \mu_i; i = 1, \dots, \kappa$, where the map to the rectangular

²⁴The question of using half or full cycles on spectral curves is purely a matter of convention. See [18, 37] for details.

²⁵The coefficients F_g^{HMM} fulfil topological recursion on a k -cut spectral curve and f_g are their double scaled analogue. This means, that the expression (3.6) should be 1-summable in the appropriate directions – In this sense one can make sense of it as a function for example by Borel-Laplace summation [51].

transseries parameters in (2.24) has the form [37]

$$\mu_i = \sigma_{i,1}\sigma_{i,2}, \quad \rho_i = \frac{\sigma_{i,1}}{\Gamma\left(1 + \frac{\mu_i}{2\pi i}\right)} e^{\alpha_i \mu_i}. \quad (3.13)$$

Here, the $\alpha_i \in \mathbb{C}$ are constants that depend on the specific choice of rectangular transseries conventions. For details we refer the interested reader to [37]. A specific choice for the parameters ρ_i and μ_i constitutes a specific choice of non-perturbative completion and we have picked the normalization in formula (3.6) to be consistent with the matrix integral results in section 2, meaning such that the trivial Stokes constants in the forward and backward direction are 1. Furthermore the partition function in formula (3.6) is given in terms of a Zak transform²⁶: All the instanton dependence has been conveniently rewritten in terms of a single sum for each involved saddle. Comments on the background independence of the expression (3.1) can be found in [48].

Let us now give some explicit checks on the above proposal by comparing to the non-perturbative contributions computed in section 2.1. We will study 3 cases, namely standard instanton contributions, negative instantons and finally their pairs:

- **Physical Sheet Instantons:** We compute the $\ell \geq 1$ instanton associated to a saddle E_i^* by picking up the ℓ mode of the Zak transform in (3.6) and normalizing by the perturbative partition function. Furthermore we are only interested in instantons, meaning for now take $\mu_i = 0$ (This implies $\rho_i \rightarrow \sigma_{i,1}$). We will restrict ourselves here to the leading order g_s contribution. Then we find

$$\begin{aligned} & \sigma_{i,1}^\ell \mathcal{Z}_G(\ell) \exp \left[\frac{\ell}{g_s} \partial_{\nu_i} f_0(\nu_1, \dots, \nu_\kappa) \Big|_{\nu_1=\dots=\nu_\kappa=0} \right] \exp \left[\frac{\ell^2}{2} \partial_{\nu_i}^2 f_0(\nu_1, \dots, \nu_\kappa) \Big|_{\nu_1=\dots=\nu_\kappa=0} \right] = \\ & = \sigma_{i,1}^\ell \mathcal{Z}_G(\ell) e^{-\ell \frac{A_i}{g_s}} \left(\frac{1}{32M'(E^*) (a - E^*)^{5/2}} \right)^{\frac{\ell^2}{2}}, \end{aligned} \quad (3.14)$$

where we have introduced the instanton action A_i exactly as in (2.6). Then formula (3.14) agrees exactly with formula (2.10). In fact up to the double scaling limit this is analogous to the computation presented in [7] and therefore the match is expected.

- **Non-Physical Sheet Instantons:** The negative instantons contained in (3.6) are new contributions so let us check them carefully: They emerge in the limit $\sigma_{i,1} \rightarrow 0$, meaning $\rho_i \rightarrow 0, \mu_i \rightarrow 0$ while $\mu_i/\rho_i = \sigma_2$, which can be seen by studying the map (3.13). We pick the $\ell = -1$ mode in the Zak transform (3.6) and expand in μ_i at lowest order to find

$$\begin{aligned} & \frac{\mathcal{Z}_G\left(-1 + \frac{\mu_i}{2\pi i}\right)}{\rho_i} \Big|_{\sigma_{i,1} \rightarrow 0} \exp \left[-\frac{1}{g_s} \partial_{\nu_i} f_0(\nu_1, \dots, \nu_\kappa) \Big|_{\nu_1=\dots=\nu_\kappa=0} \right] \times \\ & \times \exp \left[\frac{1}{2} \partial_{\nu_i}^2 f_0(\nu_1, \dots, \nu_\kappa) \Big|_{\nu_1=\dots=\nu_\kappa=0} \right] = -i \sqrt{\frac{g_s}{2\pi}} e^{\frac{A_i}{g_s}} \frac{1}{\sqrt{32M'(E^*) (a - E^*)^{5/2}}} \sigma_{i,2}. \end{aligned} \quad (3.15)$$

Again this agrees perfectly with formula (2.17). Higher order negative instantons can be computed in the same way and we checked them up to $\ell = -3$.

²⁶Partition functions as Zak transforms have some history: See for example [38, 52, 53].

- **Instanton – Non-Physical Sheet Instanton Pairs:** Last but not least we compute the mixed (1|1) sector by picking up the zero mode of the \bar{Z} ak transform (3.6) and expanding in μ to first order. We find

$$\frac{\mu}{2\pi i g_s} \partial_{\nu_i} f_0(\nu_1, \dots, \nu_\kappa) \Big|_{\nu_1=\dots=\nu_\kappa=0} = \mu \frac{i}{2\pi} \frac{A_i}{g_s}, \quad (3.16)$$

which exactly agrees with (2.19). Further checks of this type of formula are provided in [37] and we refer the interested reader to those references for details.

With this we conclude our checks on the partition function (3.6).

3.2 Choosing a Non-Perturbative Completion

To finish this discussion, let us understand the non-perturbative partition function in a more explicit setting and construct a specific non-perturbative completion: Let us start in the phase of the VMS where the free energy (2.1) is dominant. This is the analogue of the one cut phase of hermitian matrix models and the tritronquée solution of minimal strings [37], where the non-perturbative completion is given by median summation – meaning the falling instantons are turned on with the transseries parameter being half the value of their Stokes constants [31]. But in the VMS a subtlety appears: As mentioned before, the falling VMS instantons do not all live on the physical sheet of the spectral curve (see also figures 2 and 3). This means for each saddle i one has to decide if the effective potential is positive or negative and then pick the corresponding falling action: Let A_i be the action (2.6) associated to the i -th saddle point on the physical sheet. If²⁷

- $A_i > 0$: choose $\sigma_{i,1} = 1/2, \sigma_{i,2} = 0$, which translates to

$$\rho_i = \frac{1}{2}, \quad \mu_i = 0. \quad (3.17)$$

- $A_i < 0$: choose $\sigma_{i,1} = 0, \sigma_{i,2} = 1/2$, which translates to

$$\frac{\mu_i}{\rho_i} = \frac{1}{2}, \quad \rho_i \rightarrow 0, \quad \mu_i \rightarrow 0. \quad (3.18)$$

To see that this choice of initial conditions indeed only turns on falling instanton effects the reader might compare with formula (3.14) and (3.15). Interestingly, even this simple choice of non-perturbative completion already includes exponential contributions from both sheets of the spectral curve.

At this stage we should mention that the above choice of non-perturbative completion via median summation is in no way the unique possible choice²⁸: One might therefore wonder also

²⁷In this discussion we are ignoring some saddles that have 0 energy. Those will not give non-perturbative effects, but in other phases of the VMS they might modify what is meant with the perturbative sector. See also [48]. It would be interesting to investigate this further.

²⁸The choice of non-perturbative completion in a matrix model is predicated on choosing a special eigenvalue integration contour – often the contour that minimizes eigenvalue energy. But starting from this setting matrix models still exhibit various phases, where the non-perturbative completion changes through Stokes phenomena: For example study the (2, 3) - minimal string and its related cubic matrix model with potential

$$V(\lambda) = \lambda^2 - \frac{1}{6}\lambda^3,$$

about other choices of transseries parameters for the VMS where new behavior can emerge – driven by new dominant exponential contributions [37]. Let us quickly outline what to expect from the partition function (3.6) in this case: Focus on the i -th non-perturbative saddle and study a generic configuration $\rho_i \neq 0, \mu_i \neq 0$. At leading order in g_s the VMS partition function then reads

$$\begin{aligned} & \exp \left[\frac{1}{g_s^2} F_{V,0} + F_{V,0} + \dots \right] \sum_{\ell \in \mathbb{Z}} \rho_i^\ell \frac{g_s^{\ell^2/2}}{(2\pi)^{\ell/2}} G_2 \left(1 + \ell + \frac{\mu_i}{2\pi i} \right) \exp \left[\frac{1}{g_s} \left(\ell + \frac{\mu_i}{2\pi i} \right) \partial_{\nu_i} f_0 \right] \times \\ & \times \exp \left[\frac{1}{2} \left(\ell + \frac{\mu_i}{2\pi i} \right)^2 \partial_{\nu_i}^2 f_0 \right] \left(1 + g_s \left(\left(\ell + \frac{\mu_i}{2\pi i} \right) \partial_{\nu_i} f_1 + \left(\ell + \frac{\mu_i}{2\pi i} \right)^3 \partial_{\nu_i}^3 f_0 \right) + \mathcal{O}(g_s^2) \right). \end{aligned} \quad (3.19)$$

This is a modified theta function: It is a theta function sum with the extra insertion of a Barnes function $G_2(\nu)$ ²⁹. This means we should no longer expect clean exponential asymptotics [54] – but rather quasi-periodic, Zak transform like behaviour [38, 7, 37] when both parameters ρ_i and μ_i are turned on.

4 Non-Perturbative Effects in 3d Gravity

Having understood non-perturbative contributions in the VMS we want to understand their relation to 3d gravity. To be more specific, we focus on the relation between the VMS and 3d gravity on manifolds that are topologically a thickened Riemann surface $\Sigma_{g,n} \times I$ with end-of-the-world (EOW) branes at the ends of the interval: A relation that was conjectured in [55] and recently proven in [40]. For notations and conventions on 3d gravity we will follow [40]. Explicitly, the following correspondence is established³⁰

$$\mathcal{Z}_{\Sigma_{g,n} \times I}^{\text{primary}}(it_1, \dots, it_n) = e^{-\frac{\beta_1 + \dots + \beta_n}{24}} \mathcal{Z}_{g,n}(\beta_1, \dots, \beta_n), \quad (4.1)$$

where on the left hand side $\mathcal{Z}_{\Sigma_{g,n} \times I}^{\text{primary}}$ denotes the gravitational path integral on $\Sigma_{g,n} \times I$ with EOW branes and with descendants removed (see formula (2.8) of [40]). Furthermore $i \cdot t_j$ are annulus moduli for each of the n boundaries of $\Sigma_{g,n}$. On the right hand side of equation (4.1), $\mathcal{Z}_{g,n}$ is the VMS partition function on $\Sigma_{g,n}$. Lastly $\beta_i = 2\pi t_i$ are inverse temperatures and the expression still contains the $g_s = \exp(-S_0)$ dependence implicitly. This dependence is encoded on the gravity side via $1/g_s = Z_{\text{disk}}^{(a)} Z_{\text{disk}}^{(b)}$, where $Z_{\text{disk}}^{(a)}$ denotes the empty disk partition function with boundary condition a at one end of the interval I (and b on the other respectively). Conveniently $\mathcal{Z}_{g,n}$ can be computed from the VMS matrix model correlators via inverse Laplace transform

$$\mathcal{Z}_{g,n}(\beta_1, \dots, \beta_n) = \int_{\Gamma} \left(\prod_{j=1}^n \frac{du_j}{2\pi i} e^{\beta_j u_j} \right) g_s^{2g-2+n} R_{g,n}(-u_1, \dots, -u_n), \quad (4.2)$$

which has two real saddle points at $\lambda_1^* = 0, \lambda_2^* = 4$ (but none of the associated steepest descend contours are strictly real). As shown in [37] the cubic matrix model has phases where it behaves quasi-periodically – where its expansion is dominated by exponentials. In these phases the transseries parameters have values different from median summation, because the system experiences the aforementioned Stokes phenomena.

²⁹The attentive reader might be worried about the convergence properties of the instanton sum: This growth originates from the genus sum and it is discussed in detail in [37].

³⁰A comment on notation: In 3d gravity we will follow the conventions from [40] where the dependence of $1/g_s = Z_{\text{disk}}^{(a)} Z_{\text{disk}}^{(b)}$ is absorbed in the partition function. On the other hand in the VMS for the resolvent we will keep g_s explicit to be consistent with section 2: For $\mathcal{Z}_{\Sigma_{g,n} \times I}^{\text{primary}}, \mathcal{Z}_{g,n}$ we keep the dependence implicit, while for the resolvent R_i or the free energy the factors of g_s are spelled out.

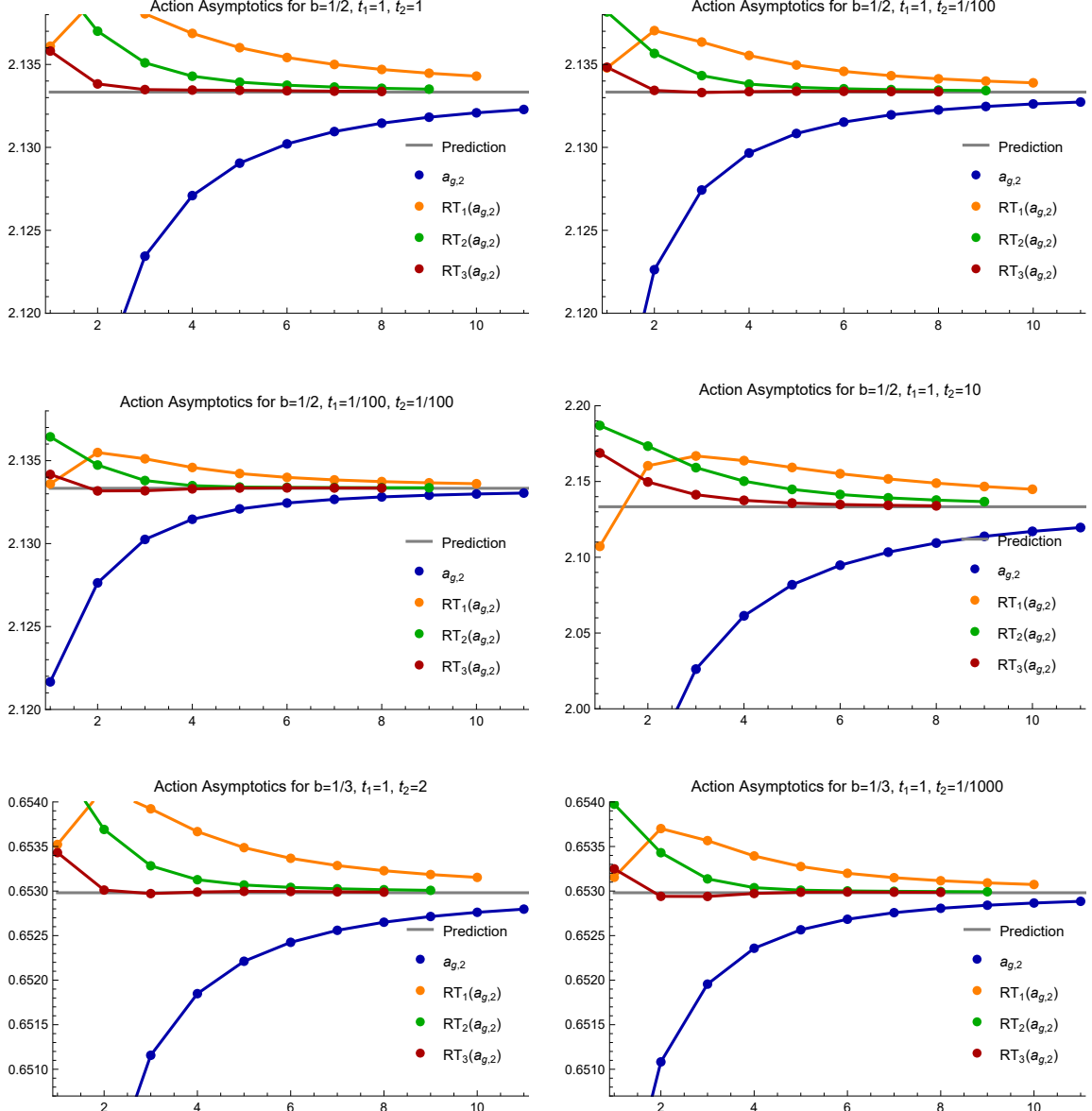


Figure 9: Asymptotic checks for the leading instanton action of the series (4.9) for various values of t_1, t_2 . Explicitly we plot the sequence $a_{g,2}(t_1, t_2)$ from formula (4.10) together with its first 3 Richardson transforms. We find good agreement with the prediction $A_{1,+}$ with a precision of around 3 digits.

where in accordance with the notation in [36] (and our previous section 2) we have made the g_s dependence for the resolvent explicit on the right hand side.

We want to understand the consequences of the sum over genus in 3d gravity with EOW branes. For this endeavour let us focus on $n = 2$ boundaries. We will start on the VMS side, where the genus sum for the resolvent reads

$$R_2(-u_1, -u_2) \simeq \sum_{g=0}^{\infty} g_s^{2g} R_{g,2}(-u_1, -u_2), \quad (4.3)$$

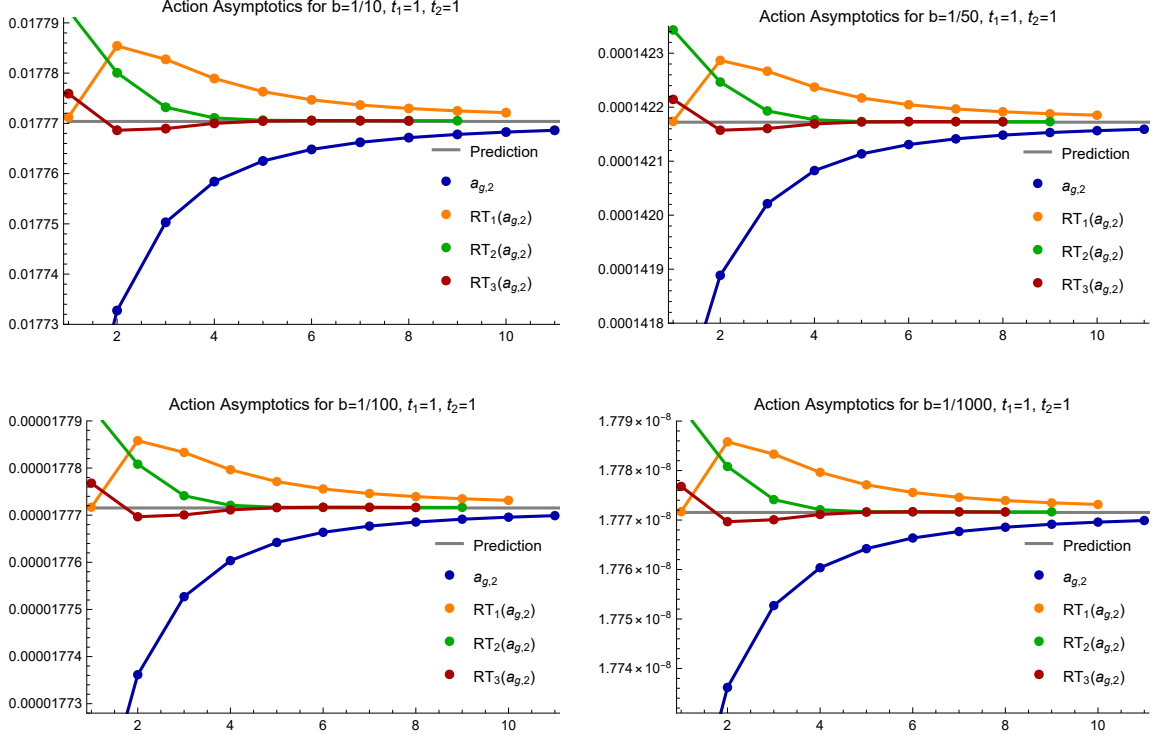


Figure 10: Asymptotic checks for the leading instanton action of the series (4.9) for increasing values of c . As in figure 9 we plot the sequence $a_{g,2}(t_1, t_2)$ from formula (4.10) together with its first 3 Richardson transforms. We find good agreement with the prediction $A_{1,+}$ with a precision of 3 relevant digits even as c increases.

and then map the results to 3d gravity via

$$\sum_{g=0}^{\infty} \mathcal{Z}_{\Sigma_{g,n=2} \times I}^{\text{primary}}(it_1, it_2) \simeq \int_{\Gamma} \left(\prod_{j=1}^2 \frac{du_j}{2\pi i} e^{\beta_j(u_j - \frac{1}{24})} \right) R_2(-u_1, -u_2). \quad (4.4)$$

Formula (4.4) can be obtained by combining (4.1) with (4.2) and switching the inverse Laplace transform with the formal genus sum. Notice again that the expansion parameter on the gravity side is given by $1/g_s = Z_{\text{disk}}^{(a)} Z_{\text{disk}}^{(b)}$ [40] and that – in the 3d gravity language – those factors are absorbed in the partition function. Consequently we need to study the non-perturbative contributions to the VMS resolvent (4.3) and understand their behaviour under the inverse Laplace transform (4.4): This is an asymptotic study in g_s and we expect the VMS resolvent transseries to include the following non-perturbative effects [10, 56, 43, 57]:

- **ZZ-type Instantons and Their Negative Siblings:** These are the standard ZZ-type instanton contributions computed in [36] and their negative siblings from section 2. For n eigenvalues and m anti-eigenvalues at each saddle point $E_{k,\pm}^*$ (see formula (2.7)) they contribute to the transseries as

$$e^{-(n-m)\frac{A_{k,\pm}}{g_s}} \tilde{R}_{E_{k,\pm}^*}^{(n|m)}(E_1, E_2) \quad (4.5)$$

where $A_{k,\pm}$ is given in (2.8) and $\tilde{R}_{E_{k,\pm}^*}^{(n|m)}(E_1, E_2)$ is an asymptotic series attached to the instanton. We want to understand what those contributions correspond to for 3d gravity – meaning after performing the inverse Laplace transform (4.4). Notice how the instanton actions in (4.5) are independent of u_1, u_2 . This means that when performing the inverse Laplace transform on (4.5) the non-perturbative exponential can be treated as just a prefactor and taken out of the integral: The instanton action does not change. Consequently we expect exactly the ZZ exponentials

$$e^{-(n-m)\frac{A_{k,\pm}}{g_s}} \quad (4.6)$$

to appear in the non-perturbative completion of the series (4.4). Exactly as in the case of the VMS they can be turned on and off by making a choice of non-perturbative completion or by crossing Stokes lines. We also emphasize again that some of the *falling* instanton contributions above come originally from the non-physical sheet of the VMS spectral curve as not all the $A_{k,\pm}$ are positive.

- **FZZT-type Instantons:** As shown in subsection 2.5 the VMS resolvents receive also non-perturbative contributions from FZZT-type exponentials (see formula (2.46))

$$e^{-\frac{\tilde{A}(E)}{g_s}}, \quad \tilde{A}(E) = 2 \int_0^E y_V(E') dE'. \quad (4.7)$$

In this context we have shown the existence of wall crossing in subsection 2.5. One might then wonder how these effects translate to the genus sum over primary partition functions in 3d gravity. For this endeavour we need to understand the effect of the inverse Laplace transform (4.4) on the action (4.7). It can be evaluated using saddle point approximation for small g_s

$$e^{-\frac{\tilde{A}(E)}{g_s}} \quad (4.8)$$

The inverse Laplace transform (4.4) localizes exactly around the saddle points of the action $\tilde{A}(u)$ in (4.7) – which correspond to the zeros of the spectral curve (2.2) given by the saddle points $E_{k,\pm}^*$. In this way the ZZ-type instanton contributions³¹ reappear. Therefore for 3d gravity the FZZT-like VMS effects produce exactly the actions $A_{k,\pm}$ in (4.6). In this sense they mix with the original ZZ-type non-perturbative effects and are no longer individually detectable. It remains to be investigated however if the wall crossing survives the transformation (4.4) by shifting around Stokes constants – meaning by jumps of the prefactors of the non-perturbative exponentials (4.6). This result is exactly consistent with similar studies for JT gravity in [43].

Summing up the above discussion we expect to find the non-perturbative exponentials (4.6) for the genus sum (4.4). To confirm this we can study the asymptotics of

$$\sum_{g=0}^{\infty} \mathcal{Z}_{\Sigma_{g,n=2} \times I}^{\text{primary}}(it_1, it_2). \quad (4.9)$$

³¹This is analogous to the FZZT-branes in minimal string theory that also localize on ZZ-branes upon integration over their moduli-space [49, 50, 18].

This is an asymptotic series in $1/g_s = Z_{\text{disk}}^{(a)} Z_{\text{disk}}^{(b)}$ and we should see the smallest ZZ instanton contribution $A_{1,+}$ leading the asymptotics, meaning

$$a_{g,2}(t_1, t_2) := \sqrt{\frac{4g^2 \mathcal{Z}_{\Sigma_{g,n=2} \times I}^{\text{primary}}(it_1, it_2)}{\left(Z_{\text{disk}}^{(a)} Z_{\text{disk}}^{(b)}\right)^2 \mathcal{Z}_{\Sigma_{g+1,n=2} \times I}^{\text{primary}}(it_1, it_2)}} \xrightarrow{g \rightarrow \infty} A_{1,+} \quad (4.10)$$

Notice the disk factors that appear in (4.10), to cancel the implicit disk dependence of the coefficients in the series (4.9). Moreover we should find the same action $A_{1,+}$ for any t_1, t_2 as any FZZT-type effects should be absent. This is indeed the case: We have computed the first 12 orders of the series (4.9) from the VMS data by using the map (4.1) and we have tested the asymptotics (4.10) for various values t_1, t_2 . The checks are visualized in figure 9 and they confirm our prediction with a precision of 3 digits.

Let us now understand the above computation in the natural language for 3d gravity, namely as an expansion in large c . Firstly we need to understand if the above asymptotic study in $1/g_s = Z_{\text{disk}}^{(a)} Z_{\text{disk}}^{(b)}$ can be carried over to the large c analysis. This is not immediate because in analogy to [10] we might expect exponential c dependence in the disk contributions [39]

$$\log\left(Z_{\text{disk}}^{(a)}\right) \sim c. \quad (4.11)$$

and in addition $\mathcal{Z}_{\Sigma_{g,n=2} \times I}^{\text{primary}}(it_1, it_2)$ is a polynomial in c at each genus g (with the disk contributions taken out). In other words the asymptotic study (4.10) is not strictly a large c analysis. Nevertheless, at large c there is a strict separation of scales between the exponential c dependence of the disk and the polynomial c dependence of the coefficients – meaning the asymptotics (4.10) should hold. In fact, we can test the asymptotics (4.10) numerically for large c (assuming the separation of scales between g_s and c ³²) which we have visualized in figure 10. We find perfect agreement of 3 relevant digits with the prediction. Concluding, we have made a strong case for the existence of the following doubly exponential contributions in c for the genus sum (4.9)

$$\exp\left[-(n-m)\frac{A_{k,\pm}}{g_s}\right], \quad (4.12)$$

where $(n|m)$ counts instantons (and negative instantons) of the type $A_{k,\pm}$ given in (4.6) with the specific formula for $A_{k,\pm}$ given in (2.8). This type of doubly exponential contribution is in line with the expectation in [39] at least for the falling exponentials. One might further wonder, if these contributions correspond to non-perturbative saddles of the gravity path integral. Lastly we should mention that a generic closed form construction of the VMS resolvents along the lines of the non-perturbative partition function in section 3 might be very useful to extend the above study past the leading instanton actions.

5 Black Hole Threshold as a Stokes Transition

Above, we have studied the resurgent properties of partition functions (and correlators) for the VMS and 3d gravity. What we have not discussed yet is the eigenvalue density. More specifically we want to understand how non-perturbative effects behave as we cross the edge of the eigenvalue

³²Of course this is not a proper large c analysis, but it gives us confidence that the limit $c \rightarrow \infty$ does not break the asymptotics (4.10).

distribution in matrix models. For the setting with a generic double scaled spectral curve as given in formula (2.4) compute the resolvent

$$R(E) = \left\langle \text{Tr} \frac{1}{E - M} \right\rangle, \quad (5.1)$$

and study the density of states on the real line [58, 10]

$$\langle \varrho(E) \rangle = -\frac{1}{2\pi i} \text{Disc} [R(E)] = -\frac{1}{2\pi i} \lim_{\epsilon \rightarrow 0} (R(E + i\epsilon) - R(E - i\epsilon)), \quad E \in \mathbb{R}. \quad (5.2)$$

We want to investigate the behavior of the density as the threshold $E = 0$ is crossed. In this context the following leading behavior was proposed in [10]

$$\langle \varrho(E) \rangle \simeq \begin{cases} \frac{1}{g_s} \varrho_0(E) - \frac{1}{4\pi E} \cos \left(\frac{2\pi}{g_s} \int_0^E dE' \varrho_0(E') \right), & E > 0, \\ -\frac{1}{8\pi E} \exp \left(-\frac{2}{g_s} \int_0^E dE' y(E') \right), & E < 0, \end{cases} \quad (5.3)$$

where $\varrho_0(E)$ is the classical part of the density (5.2). In the following we will generalize this result from a resurgent viewpoint and understand it in terms of Stokes and anti-Stokes transitions. We will further show that (5.3) is the universal piece of a more generic expression that depends on a choice of non-perturbative completion. We will first present the generic construction for any hermitian matrix model followed by two examples: firstly we discuss implications for the VMS and for 3d gravity and secondly we comment on JT gravity.

5.1 Generic Construction

We want to understand how non-perturbative effects correct the eigenvalue density (5.2), which is obtained from the resolvent by taking the discontinuity along the real line [10]. Consequently let us start with the generic matrix model resolvent (2.45) and construct the resurgent non-perturbative completion for the asymptotic series in g_s . Such effects have been computed in [10, 56, 57] and we have already seen them in the VMS explicitly in subsection 2.5. Famously there are two types of non-perturbative effects:

- **FZZT Contributions** whose leading order for the action on the physical sheet was computed in [10, 56, 57] and reads³³

$$R^{\text{FZZT}-}(E) \simeq \left(\frac{i}{4E} + \mathcal{O}(g_s) \right) e^{-\frac{\tilde{A}(E)}{g_s}} \quad (5.4)$$

where (see equation (2.46) for the VMS analogue)

$$\tilde{A}(E) = 2 \int_0^E y(E') dE'. \quad (5.5)$$

On the other hand, on the non-physical sheet we have

$$R^{\text{FZZT}+}(E) \simeq \left(-\frac{i}{4E} + \mathcal{O}(g_s) \right) e^{\frac{\tilde{A}(E)}{g_s}} \quad (5.6)$$

Here there are no towers of multiples of the FZZT action.

³³Notice that the result for the FZZT effects is normalized to match matrix integral computations [57].

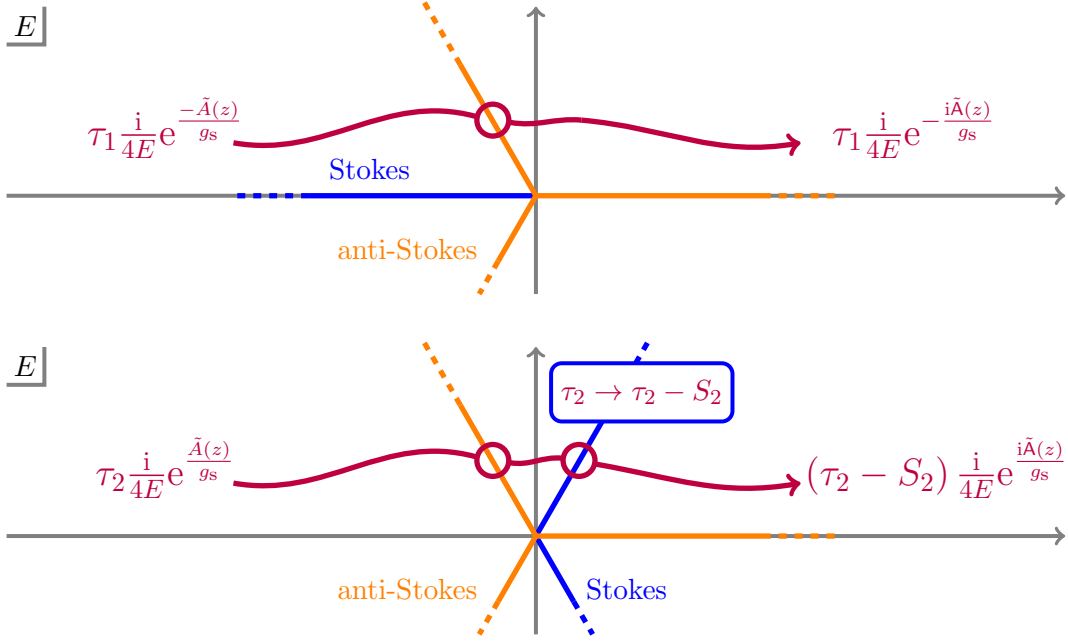


Figure 11: We show the analytic continuation of FZZT-branes from the region $E < 0$ to $E > 0$ in a neighbourhood of the origin. We focus on the transition above the real line (5.18). Start in the upper graphic with the falling FZZT contribution shown: We have a Stokes line (blue) on the negative real line and anti-Stokes lines (orange) emanating from the origin in the directions $0, \frac{2}{3}\pi$ and $\frac{4}{3}\pi$. Then when moving from left to right the instanton action will experience the effects of the anti-Stokes lines and change from exponentially damped to oscillating. Compare this picture with the graphic below that depicts the growing exponential: Now there are Stokes lines (blue) in the directions $\frac{1}{3}\pi$ and $\frac{5}{3}\pi$, and the anti-Stokes lines (orange) remain unchanged. Now when moving from left to right the action still changes dominance same as before, but on top of it we are passing a Stokes line, which shifts τ_2 to $\tau_2 - S_2$.

- **ZZ Contributions** that are associated to saddle points of the effective action. For a saddle E^* we have the one (anti-) instanton contribution at leading order [43] (compare with (2.5))

$$R^{(1|0)zz}(E) \simeq e^{-\frac{\tilde{A}(E^*)}{g_s}} \left(\frac{1}{4} \sqrt{\frac{g_s}{4\pi M'(E^*)(a - E^*)^{\frac{5}{2}}}} \sqrt{\frac{E^*}{-E} \frac{1}{E - E^*}} + \mathcal{O}(g_s^{3/2}) \right), \quad (5.7)$$

$$R^{(0|1)zz}(E) \simeq i e^{\frac{\tilde{A}(E^*)}{g_s}} \left(\frac{1}{4} \sqrt{\frac{g_s}{4\pi M'(E^*)(a - E^*)^{\frac{5}{2}}}} \sqrt{\frac{E^*}{-E} \frac{1}{E - E^*}} + \mathcal{O}(g_s^{3/2}) \right), \quad (5.8)$$

where $A(E)$ is given in formula (5.5). Each ZZ contribution of course comes with an infinite tower of siblings associated with the number of n eigenvalues and m anti eigenvalues that tunnel to x^* . Generically we then denote the ZZ contributions by $R^{(n|m)zz}(E)$.

Putting the above contributions together we can write the generic transseries for the resolvent. In general it will contain all the possible combinations of ZZ- and FZZT-branes, as shown in [57]. However we are interested in the resurgent behaviour as the threshold $E = 0$ is crossed, meaning we want to study the instanton actions that depend on E : the FZZT-branes (5.4) and (5.6). In

other words we focus on the pure FZZT subsector of the transseries that reads³⁴

$$R(E, \tau_1, \tau_2) \simeq \sum_{g=0}^{\infty} R_g(E) g_s^{2g-1} + \tau_1 R^{\text{FZZT}_-}(E) + \tau_2 R^{\text{FZZT}_+}(E), \quad (5.9)$$

where $\tau_1, \tau_2 \in \mathbb{C}$ are the FZZT transseries parameters whose choice fixes a non-perturbative completion³⁵. Let us now understand the resurgent behaviour of the transseries (5.9) around $E = 0$. Specifically we want to understand (anti-) Stokes transitions. For this endeavour focus on a small neighbourhood \mathcal{U} of the origin $E = 0$, where the action (5.5) behaves as³⁶

$$\tilde{A}(E) \sim (-E)^{3/2}, \quad E \in \mathcal{U}. \quad (5.10)$$

For \mathcal{U} sufficiently small this is a good approximation. Then the Stokes and anti-Stokes lines in a neighbourhood of the origin are³⁷

- **Stokes Lines** given by

$$\text{Im} \left(\tilde{A}(E) \right) = 0, \quad (5.11)$$

with $\text{Re} \left(\tilde{A}(E) \right) > 0$. Study first the physical sheet FZZT action $\exp \left(-\tilde{A}(E)/g_s \right)$: It has only one Stokes line emanating from $E = 0$ in the π direction. Take $\mathbf{E} \in \mathbb{R}_{<0}$ such that $\mathbf{E} \pm i\epsilon \in \mathcal{U}$ with $\epsilon > 0$ and small: The Stokes line is then crossed as

$$R(\mathbf{E} + i\epsilon, \tau_1, \tau_2) \longrightarrow R(\mathbf{E} - i\epsilon, \tau_1 + S_1, \tau_2), \quad (5.12)$$

where we have introduced the Stokes constant $S_1 = 1$. Notice how it is normalized to the identity. This is because the transseries sectors are normalized to agree exactly with eigenvalue tunnelling – which corresponds in turn exactly to Stokes transitions (for details see [6, 7, 15]). Now turn to the action on the non-physical sheet $\exp \left(\tilde{A}(E)/g_s \right)$: Here we find two Stokes lines emanating from $E = 0$ in the directions $\pi/3$ and $-\pi/3$. See figure 11 for a visualization. Consider now $\mathbf{E}_+ = \mathbf{E} \exp \left(i\frac{\pi}{3} \right)$, $\mathbf{E}_- = \mathbf{E} \exp \left(i\frac{5\pi}{3} \right)$, $\mathbf{E} \in \mathbb{R}$ such that $\mathbf{E}_+ \exp(\pm i\epsilon) \in \mathcal{U}$ and $\mathbf{E}_- \exp(\pm i\epsilon) \in \mathcal{U}$ for small and real positive ϵ . Then we can cross the Stokes lines via

$$R(\mathbf{E}_+ e^{+i\epsilon}, \tau_1, \tau_2) \longrightarrow R(\mathbf{E}_+ e^{-i\epsilon}, \tau_1, \tau_2 - S_2), \quad (5.13)$$

$$R(\mathbf{E}_- e^{-i\epsilon}, \tau_1, \tau_2) \longrightarrow R(\mathbf{E}_- e^{+i\epsilon}, \tau_1, \tau_2 + S_2), \quad (5.14)$$

where the Stokes constant reads $S_2 = 1$ as expected by now and the extra minus sign of the shift in the first line comes from the direction of travel through the Stokes line.

- **Anti-Stokes Lines** given by

$$\text{Re} \left(\tilde{A}(E) \right) = 0 \quad (5.15)$$

³⁴We comment on the inclusion of ZZ-branes towards the end of this subsection.

³⁵Of course the ZZ exponentials come attached with their own transseries parameters so for a complete non-perturbative completion one also has to fix those on top of the FZZT parameters mentioned here.

³⁶Notice that in order to compute the density (5.2) we need to understand the resolvent in a neighbourhood of the real line, because we have to take a discontinuity: Even if we are only interested in the density strictly on the real line we need to understand the behaviour of the resolvent also slightly away from it.

³⁷Often the nomenclature for (anti-) Stokes lines in the mathematical literature differs from the one in physics: What is an anti-Stokes line here is a Stokes line in the mathematics literature.

which are the lines where exponentials that were previously suppressed become dominant or vice versa. From $E = 0$ they emanate to the directions $0, 2\pi/3, 4\pi/3$ for both FZZT actions. See again figure 11 for a visualization.

We can assemble the above Stokes and anti-Stokes transitions into the local picture close to the threshold $E = 0$ depicted in figure 11. Armed with this discussion we are now ready to compute non-perturbative contributions to the density by analysing the discontinuity (5.2). We first focus on $E < 0$: Here there is a discontinuity that is created by the Stokes line on the negative real axis, which we can compute from formula (5.12) to read

$$\frac{1}{2\pi i} \text{Disc} [R(E, \tau_1, \tau_2)] \simeq \underbrace{S_1}_{=1} \left(\frac{1}{8\pi E} + \mathcal{O}(g_s) \right) e^{-\frac{\tilde{A}(E)}{g_s}}, \quad E < 0. \quad (5.16)$$

Notice that this result does not depend on the non-perturbative completion (the transseries parameters). Notice also how this discontinuity comes purely from the Stokes transition on the negative real line: It is expected to be smoothed out by resumming higher g_s contributions. It is also worthwhile to mention that only the damped exponential appears here because this is the one that experiences a Stokes line on the negative real axis – in contrast to the growing exponential, which does not: This is intrinsic to the construction of the density (5.2) and not an external choice that we had to make. There are no further contributions to the discontinuity in the region $E < 0$. Consequently move to $E > 0$. We will proceed by considering continuous paths starting from $E < 0$ and keep track of the changes as we move to $E > 0$ (see figure 11). The FZZT contributions will experience an anti Stokes line as they cross close to $E = 0$ and for this reason they will change dominance. Moreover, in the case considered here where the spectral curve is strictly real or imaginary on the real line, the FZZT action becomes purely imaginary close to the positive real line. This anti-Stokes phenomenon is exactly what drives the change of behaviour from exponential for $E < 0$ to oscillating for $E > 0$. Above the real line let us use the offset $E = E + i\epsilon$ and imply ϵ to be small. We will then write

$$i\tilde{A}(E) = \lim_{\epsilon \rightarrow 0} \tilde{A}(E + i\epsilon), \quad E \in \mathbb{R}_{>0}. \quad (5.17)$$

Following the path drawn in figure 11 – above the real line – then amounts to

$$\begin{array}{ccc} \underline{E = E + i\epsilon, E < 0 :} & & \underline{E = E + i\epsilon, E > 0 :} \\ \tau_1 \left(\frac{i}{4E} + \mathcal{O}(g_s) \right) e^{-\frac{\tilde{A}(E)}{g_s}} & \xrightarrow{\text{(Figure 11)}} & \tau_1 \left(\frac{i}{4E} + \mathcal{O}(g_s) \right) e^{-\frac{i\tilde{A}(E)}{g_s}}, \\ \tau_2 \left(-\frac{i}{4E} + \mathcal{O}(g_s) \right) e^{+\frac{\tilde{A}(E)}{g_s}} & & (\tau_2 - S_2) \left(-\frac{i}{4E} + \mathcal{O}(g_s) \right) e^{+\frac{i\tilde{A}(E)}{g_s}}, \end{array} \quad (5.18)$$

where the first line corresponds to the physical sheet FZZT contribution (5.4), whereas the second line shows the change of the non-physical sheet one (5.6). Further we remember that $S_2 = 1$. In the same spirit we can follow the path below the real line, which yields

$$\begin{array}{ccc} \underline{E = E - i\epsilon, E < 0 :} & & \underline{E = E - i\epsilon, E > 0 :} \\ \tau_1 \left(\frac{i}{4E} + \mathcal{O}(g_s) \right) e^{-\frac{\tilde{A}(E)}{g_s}} & \xrightarrow{\hspace{2cm}} & \tau_1 \left(\frac{i}{4E} + \mathcal{O}(g_s) \right) e^{+\frac{i\tilde{A}(E)}{g_s}}, \\ \tau_2 \left(-\frac{i}{4E} + \mathcal{O}(g_s) \right) e^{+\frac{\tilde{A}(E)}{g_s}} & & (\tau_2 + S_2) \left(-\frac{i}{4E} + \mathcal{O}(g_s) \right) e^{-\frac{i\tilde{A}(E)}{g_s}}, \end{array} \quad (5.19)$$

where again the first line corresponds to the physical sheet FZZT and the second line to its sibling and again $S_2 = 1$. Then the FZZT contribution to the discontinuity for $E > 0$ reads

$$\underbrace{S_2}_{=1} \left(\frac{i}{2E} + \mathcal{O}(g_s) \right) \cos \left(\frac{\tilde{A}(E)}{g_s} \right) - (\tau_2 + \tau_1) \left(\frac{1}{2E} + \mathcal{O}(g_s) \right) \sin \left(\frac{\tilde{A}(E)}{g_s} \right). \quad (5.20)$$

Interestingly the cosine part only depends on Stokes constants, while the sine part depends on transseries parameters! We are now in a position to put together all of the above contributions to find the non-perturbative density at leading order in g_s

$$\langle \varrho(E, \tau_1, \tau_2) \rangle \simeq \begin{cases} \frac{1}{g_s} \varrho_0(E) - \frac{1}{4\pi E} \cos \left(\frac{\tilde{A}(E)}{g_s} \right) + (\tau_2 + \tau_1) \frac{i}{4\pi E} \sin \left(\frac{\tilde{A}(E)}{g_s} \right), & E > 0, \\ -\frac{1}{8\pi E} \exp \left(-\frac{A(E)}{g_s} \right), & E < 0. \end{cases} \quad (5.21)$$

Some comments are in order: Firstly, the expression (5.21) is just the leading term of a full transseries that is still asymptotic and should be resummed to find the non-perturbative density as a function. Secondly, the oscillatory behaviour of the non-perturbative density (5.21) for $E > 0$ comes from FZZT-branes that have undergone Stokes and anti-Stokes transitions³⁸ as computed in (5.18). We identify³⁹



Thirdly, the universal piece – meaning the τ_1, τ_2 independent piece – of formula (5.21) corresponds exactly to the result (5.3) from [10]. Indeed starting from the explicit form for the spectral curve (2.4) we can use the definition of the density (5.2) to find

$$\tilde{A}(E) = 2\pi \int_0^E \varrho_0(E') dE'. \quad (5.22)$$

Notice furthermore, that in contrast to the computation in [10] no particular choice of matrix integral contour was needed to obtain the aforementioned universal piece – in fact it is *universally* there for any choice of non-perturbative completion. On top of this, there are further contributions that do depend on the transseries parameters τ_1, τ_2 – and it is only here where the choice of non-perturbative completion enters. These non-universal terms are still oscillatory – in fact they are of order $\mathcal{O}(1)$ and in this sense cannot be ignored when turned on. Last but not least, let us again comment on the fact that the discontinuity of the resolvent on the negative real line is mitigated by a Stokes transition, which implies the expectation that it should be smoothed out by g_s corrections upon resummation of the asymptotic perturbative series. In this sense the full non-perturbative eigenvalue density is still expected to vanish in the region $E < 0$. Let us finish this subsection with two comments:

³⁸Anti-Stokes transitions are sometimes related to phase transitions [8, 37, 59]. It could be interesting to explore this connection further.

³⁹This is interesting to study because of the following analogy: In JT gravity, oscillatory terms in the matrix model density might indicate that any exact microscopic realization (like a single hamiltonian system drawn from the ensemble) should have a discrete spectrum [60, 10, 61].

Universality of Oscillatory Behaviour: We want to elaborate on the fact, that formula (5.21) has a universal piece that emerges purely from Stokes transitions. It comes about as follows: even when initially turning off all non-perturbative FZZT contributions (choosing $\tau_1 = \tau_2 = 0$ for the resolvent), the Stokes transitions at $E = 0$ will turn them back on and generate oscillatory behaviour for the density. In other words such oscillations should appear in the density for any hermitian matrix model *independent of the choice of non-perturbative completion*. The resurgence machinery above constructs them automatically: They do not need to be put in by hand, be it by choice of eigenvalue integration contour or by choice of transseries parameters. In this context let us further remark that the minimal choice (where all FZZT instanton effects are initially turned off, meaning $\tau_1 = \tau_2 = 0$) exactly produces the same result as in [10] where it was obtained by choosing a real eigenvalue integration contour. As a final comment, formula (5.21) was derived for generic hermitian matrix models: It is therefore natural to conjecture that it holds for any problem that fulfils topological recursion. In fact, our construction above does not rely on an explicit matrix integral formulation – it is based purely on the non-perturbative structure of the resolvent.

Inclusion of ZZ-Branes: Finally, let us comment on ZZ-brane contributions. For simplicity we focus our attention on the one instanton and anti-instanton contributions (5.7) and (5.8) for a saddle point E^* . They contribute additively to the transseries (5.9) with

$$\sigma_1 R^{(1|0)zz}(E) + \sigma_2 R^{(0|1)zz}(E), \quad (5.23)$$

where σ_1, σ_2 are the ZZ transseries parameters. Notice that the instanton actions $A_{k,\pm}$ are E independent, meaning in contrast to the FZZT analysis above there are no Stokes transitions when varying E . Nevertheless, the explicit expressions for the ZZ instantons (5.8) and (5.7) have square root branch cuts on the positive real line – where they will contribute to the discontinuity of the resolvent (5.2) (meaning to the density). Then we simply study

$$\frac{1}{2\pi i} \text{Disc} \left[\sigma_1 R^{(1|0)zz}(E) \right] \simeq \begin{cases} 0, & E \leq 0, \\ \sigma_1 \frac{1}{\pi i} R^{(1|0)zz}(E), & E > 0, \end{cases} \quad (5.24)$$

$$\frac{1}{2\pi i} \text{Disc} \left[\sigma_2 R^{(0|1)zz}(E) \right] \simeq \begin{cases} 0, & E \leq 0, \\ \sigma_2 \frac{1}{\pi i} R^{(0|1)zz}(E), & E > 0. \end{cases} \quad (5.25)$$

We can see that there is no contribution in the region $E < 0$ which is expected. After crossing the threshold $E = 0$ the ZZ-branes are turned back on⁴⁰ with two times the transseries parameters as compared to the resolvent transseries. We expect similar results for higher $(n|m)$ contributions, but there the switching of square root sheets might not have the simple effect of the factor of 2 above. Nevertheless, because of the absence of square root branch cuts on the negative real line, we do not expect any ZZ contribution to appear for $E < 0$ even for higher $(n|m)$ ZZ contributions. It would be interesting to study the contributions of all ZZ-branes in more detail, especially those that appear together with the FZZT contributions (see also [57]).

5.2 Example: The Virasoro Minimal String and 3d Gravity

We want to check the above derivation on the example of the VMS and understand possible implications for 3d gravity as introduced in section 4. Let us first focus on the VMS and understand the discussion in subsection 5.1 in that context. To give the explicit formula for the

⁴⁰They are turned on by the discontinuity of the square-root, not by a Stokes phenomenon.

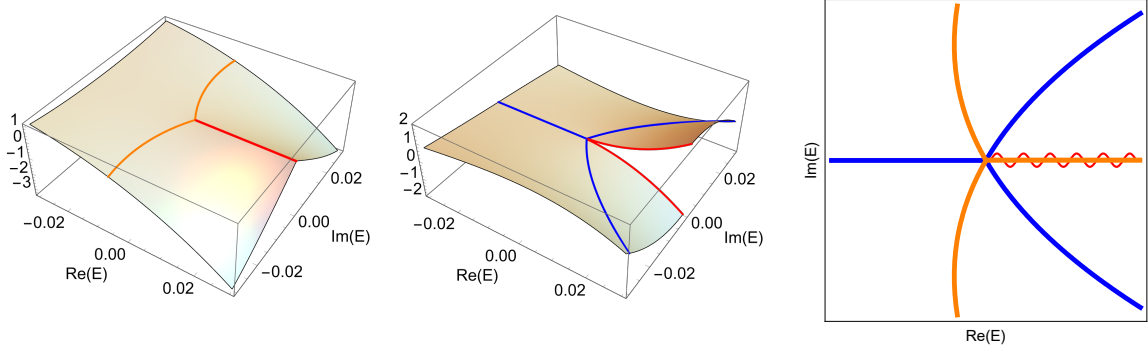


Figure 12: We plot the effective potential of the VMS as a function of E . On the left we show the real part with the anti-Stokes lines in orange, in the middle we show the imaginary part together with Stokes lines in blue, and on the right we show the complex E plane with both types of Stokes transitions drawn. In all figures we denote the branch cut on the positive real line in red. Close to $E = 0$ we indeed find the exact Stokes behaviour as predicted in the generic case of subsection 5.1 as shown in figure 11.

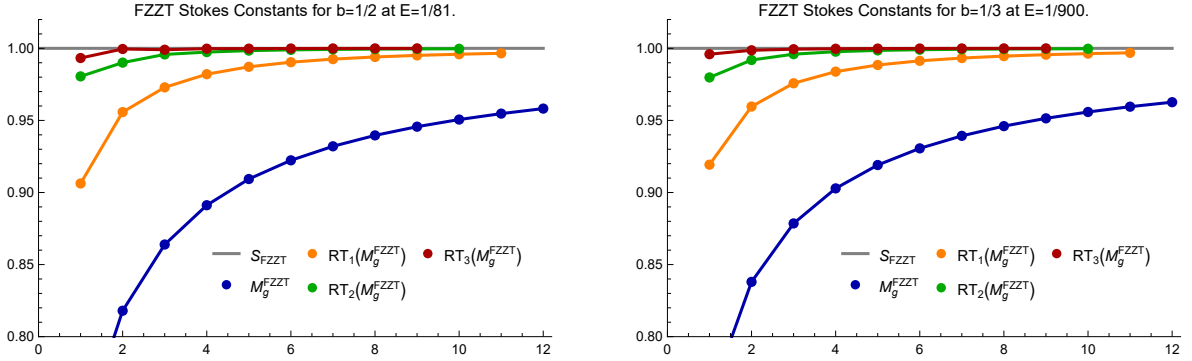


Figure 13: Asymptotic checks for the Stokes constants of the FZZT contributions. Here we plot the sequence (5.27) and check its asymptotic behaviour. We depict the sequence itself together with its first 3 Richardson transforms. We find perfect agreement with the prediction.

non-perturbative completion of the VMS density we need the FZZT instanton action $\tilde{A}(E)$ given in formula (2.46) and we further compute the action $\tilde{\tilde{A}}(E)$ given in formula (5.17) to be

$$\tilde{\tilde{A}}(E) = \frac{2\sqrt{2}b}{b^4-1} \left((1+b^2) \sinh \left[2\pi \left(b - \frac{1}{b} \right) \sqrt{-E} \right] + (1-b^2) \sinh \left[2\pi \left(b + \frac{1}{b} \right) \sqrt{-E} \right] \right). \quad (5.26)$$

Let us start by studying the FZZT instanton action (2.46) close to the origin $E = 0$. To this end we have visualized the effective potential of the VMS in figure 12. Indeed close to the origin the Stokes graph matches exactly to the discussion in subsection 5.1 with expected deviation as we move further out into the E plane (see also figure 11).

We can furthermore check the Stokes constants $S_1 = 1$ in formula (5.12) and $S_2 = 1$ in formulae (5.14) and (5.13) explicitly with large order methods. We are interested in the region

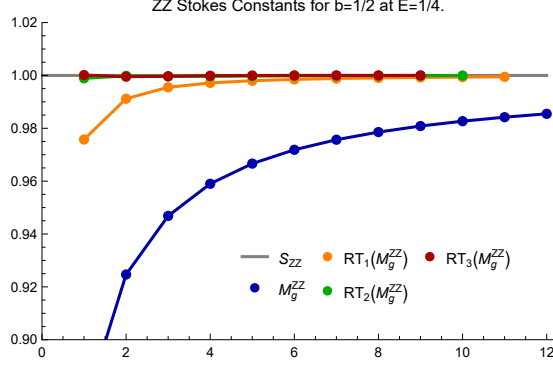


Figure 14: Asymptotic checks for the Stokes constants of the ZZ contributions. We plot the sequence (5.27) and check its asymptotic behaviour. We depict the sequence itself together with its first 3 Richardson transforms and perfect agreement with the prediction. Compare this asymptotic check with the FZZT check visualised in figure 13.

$E > 0$, where have the prediction (see also subsection 2.5 for the $E < 0$ discussion)

$$\begin{cases} M_g^{\text{FZZT}}(E, b) := \pi \frac{R_g(E) \tilde{A}(E)^{2g-1}}{\Gamma(k-1)} \{4E\} & \xrightarrow{g \rightarrow \infty} 1, \quad \tilde{A}(E) < A, \\ M_g^{\text{ZZ}}(E, b) := \pi \frac{R_g(E) A^{2g-\frac{3}{2}}}{\Gamma(k-\frac{3}{2})} \left\{ 2^{7/4} \pi^{3/2} \sqrt{b \sin(b^2 \pi)} \frac{\sqrt{E(b^2-4E)}}{b} \right\} & \xrightarrow{g \rightarrow \infty} 1, \quad \tilde{A}(E) \geq A. \end{cases} \quad (5.27)$$

Here the first line corresponds to the FZZT contribution while the second line is the standard ZZ prediction (compare also to (2.47) in subsection 2.5). We have checked these asymptotics with the available data (up to genus 14 as in subsection 2.5) with 3 digits of precision. The checks are visualized in figures 13 and 14. In addition we can compute the Stokes constants by Borel-Laplace summing and checking the discontinuity across the Stokes line. Explicitly, we will compute the Borel transform, approximate it with a Padé approximant and compute the residues of poles when crossing each of the Stokes lines (For similar techniques see [28, 62, 47, 63]). We choose $b = \frac{1}{2}$. Further we have chosen small values $z = -0.1, z = 0.0560049 \mp 0.114615i$ that lie on each Stokes line respectively⁴¹. In this way we find

$$\text{Stokes line at } \arg(E) = \pi : \quad S_1 = 0.9139 \dots, \quad (5.28)$$

$$\text{Stokes line at } \arg(E) = \frac{\pi}{3} : \quad S_2 = 0.9577 \dots - 0.0061 \dots i, \quad (5.29)$$

$$\text{Stokes line at } \arg(E) = \frac{4\pi}{3} : \quad S_2 = 0.9577 \dots + 0.0061 \dots i. \quad (5.30)$$

Given that we have only 14 terms in the resolvent series, this shows good agreement with the predictions of $S_1 = S_2 = 1$ in subsection 5.1. Based on the Stokes network in figure 12 and the numerical checks for the Stokes constants we conclude that the analysis in subsection 5.1 applies to the VMS verbatim and we find exactly formula (5.21) which we specialize to the VMS case

⁴¹Notice that the Stokes lines for the VMS deform slightly when moving away from the origin and they no longer lie cleanly on the rays $\frac{1+2k}{3}$. Therefore we have numerically computed values of z that hit the Stokes lines exactly.

below

$$\langle \varrho_V(E, \tau_1, \tau_2) \rangle \simeq \begin{cases} \frac{1}{g_s} \varrho_{V,0}(E) - \frac{1}{4\pi E} \cos\left(\frac{\tilde{A}(E)}{g_s}\right) + (\tau_2^V + \tau_1^V) \frac{i}{4\pi E} \sin\left(\frac{\tilde{A}(E)}{g_s}\right), & E > 0, \\ -\frac{1}{8\pi E} \exp\left(-\frac{A(E)}{g_s}\right), & E < 0. \end{cases} \quad (5.31)$$

Let us briefly discuss the structure of that formula: This is the leading order of a transseries – meaning the involved series are still asymptotic. $\varrho_{V,0}$ is the leading order of the perturbative VMS density and $\tilde{A}(E)$ is the FZZT contribution after anti-Stokes transition given in (5.26). In the non-perturbative VMS density (5.31) there is a falling exponential term on the negative real line. On the other hand oscillatory terms are turned on when crossing the Stokes and anti-Stokes lines at the origin $E = 0$. Then, for $E > 0$ we find a universal contribution coming from Stokes constants and an additional piece that depends on the non-perturbative completion (choosing τ_1^V, τ_2^V). To keep the density real we should choose $\text{Re}(\tau_1 + \tau_2) = 0$. As expected this is exactly analogous to the generic result (5.21).

Let us now understand the connection to 3d gravity: We will again employ the setting of [40] as already described in section 4, where the gravitational path integral on $\Sigma_{g,n} \times I$ with EOW branes at the ends of the interval I is identified with correlators of the VMS. We can compute the 3d gravity primary density $\rho_{\text{grav}}^{(ab)}(h)$ as an integral of the disk partition function [40]

$$\left\langle \rho_{\text{grav}}^{(ab)}(h) \right\rangle_{g=0} = \int_{\Gamma} \frac{d\beta}{2\pi i} e^{\beta(h - \frac{c-1}{24})} Z_{\text{Disc}}(\beta) = \frac{2\sqrt{2}}{P} \sinh(2\pi b P) \sinh(2\pi b^{-1} P) \Big|_{P^2 = h - \frac{c-1}{24}}, \quad (5.32)$$

where the contour $\Gamma = \gamma + i\mathbb{R}, \gamma \in \mathbb{R}_{>0}$. Here a, b correspond to the boundary conditions of the EOW branes at the end of the interval I and h is a primary conformal weight. The brackets $\langle \dots \rangle$ on the gravity side denote ensemble averaging and the subscript selects a genus. As in [40] (and as reviewed in section 4) the disk factors and the string coupling at each genus are implicit in this formulation and we have the identification $1/g_s = Z_{\text{disk}}^{(a)} Z_{\text{disk}}^{(b)}$. The density shows Cardy behavior for $h > \frac{c-1}{24}$ ⁴². We now use the map from [40]

$$\left\langle \rho_{\text{grav}}^{(ab)}(h) \right\rangle_g = \langle \varrho_V(E) \rangle_g \Big|_{E = h - \frac{c-1}{24}}, \quad (5.33)$$

where for the VMS quantities $\langle \dots \rangle$ denotes the matrix model expectation value and the subscript g selects a genus in the perturbative expansion. It is then straightforward to identify the onset of the Cardy behaviour with the threshold $E = 0$ in the VMS matrix model – exactly where the FZZT-branes undergo Stokes and anti-Stokes transitions (see also figure 12). With this machinery in place, we can now try to understand the non-perturbative effects that arise if one sums the 3d gravity density over the genus. Consequently, sum equation (5.33) over g to form the following asymptotic equality

$$\langle \varrho_V(E) \rangle \Big|_{E = h - \frac{c-1}{24}} \xrightarrow[\text{expansion}]{\text{asymptotic}} \sum_{g=0}^{\infty} \langle \varrho_V(E) \rangle_g \Big|_{E = h - \frac{c-1}{24}} = \sum_{g=0}^{\infty} \left\langle \rho_{\text{grav}}^{(ab)}(h) \right\rangle_g, \quad (5.34)$$

⁴²We can expand (5.32) at large P to find

$$\exp\left(2\pi\sqrt{\frac{c-1}{6}}\sqrt{h - \frac{c-1}{24}}\right).$$

where we have written a true equality between the two asymptotic series, because they are really equal term by term. One can now wonder about their non-perturbative completion: First choose $1/g_s = Z_{\text{disk}}^{(a)} Z_{\text{disk}}^{(b)}$ as organizing parameter for the asymptotic study⁴³. Secondly, because the VMS and the gravity sum in formula (5.34) are really exactly identical, they will have the exact same asymptotic behaviour⁴⁴ and therefore they will also generate the exact same transseries – the only free choice being the transseries parameters. This choice is where the VMS non-perturbative completion (with parameters τ_1^V, τ_2^V) might differ from the completion of the gravity sum in (5.34), where we will therefore introduce new transseries parameters $\tau_1^{\text{grav}}, \tau_2^{\text{grav}}$ ⁴⁵. Consequently we employ formula (5.31) for $E > 0$ to find at leading order

$$\begin{aligned} \left\langle \rho_{\text{grav}}^{(ab)}(h) \right\rangle_0 &= \frac{1}{4\pi \left(h - \frac{c-1}{24}\right)} (1 + \mathcal{O}(g_s)) \cos\left(\frac{\tilde{A}\left(h - \frac{c-1}{24}\right)}{g_s}\right) + \\ &+ (\tau_2^{\text{grav}} + \tau_1^{\text{grav}}) \frac{i}{4\pi \left(h - \frac{c-1}{24}\right)} (1 + \mathcal{O}(g_s)) \sin\left(\frac{\tilde{A}\left(h - \frac{c-1}{24}\right)}{g_s}\right), \end{aligned} \quad (5.35)$$

where $\tilde{A}(E)$ is given in formula (5.26). Interestingly formula (5.35) still contains a universal, oscillating piece, that is inherited from the VMS description. On top of this we also have oscillatory terms that depend on the gravity transseries parameters.

To summarize, the non-perturbative VMS density receives oscillatory contributions of order $\mathcal{O}(1)$ (universal and τ_1^V, τ_2^V dependent) from FZZT-branes that have experienced an anti-Stokes transition at the threshold $E = 0$. On the 3d gravity (with EOW branes) side we can say that if one sums the primary density over the genus one finds similar oscillatory contributions. Here again there is a universal part and one that depends on the parameters $\tau_1^{\text{grav}}, \tau_2^{\text{grav}}$. A priori it is not clear if one is supposed to set $\tau_1^{\text{grav}} = \tau_1^V, \tau_2^{\text{grav}} = \tau_2^V$. Nevertheless, it would be interesting to construct a full non-perturbative completion of the density along the lines of section 3 and [37] to exactly quantify the non-perturbative "freedom" inherent to the construction above⁴⁶.

5.3 Example: JT Gravity

We want to further comment on JT gravity. As a limit of the VMS the above discussion clearly also applies here. We will follow the conventions of [43], which is exactly consistent with double scaling the VMS⁴⁷ results computed above in the conventions of [36]. At the same time, non-perturbative JT gravity has been discussed at length in the literature. Therefore some g_s corrections to formula (5.4) and (5.6) are known explicitly for this example and we can compute higher order corrections to our generic formula (5.21). Namely we have the FZZT prediction [56, 43, 57]

$$R^{\text{FZZT-}}(E) \simeq \frac{i}{4E} \left(1 - g_s \frac{17 - 2\pi^2 E}{12(-E)^{3/2}} - g_s^2 \frac{1225 - 644\pi^2 E + 148\pi^4 E^2}{288E^3} + \dots \right) e^{-\frac{\tilde{A}(E)}{g_s}}, \quad (5.36)$$

⁴³Similar to the discussion in section 4 it is not straightforward to disentangle the large c growth of $1/g_s = Z_{\text{disk}}^{(a)} Z_{\text{disk}}^{(b)}$ and the c dependence of the density itself. For the current discussion and based on our explicit checks in section 4 let us assume that this procedure is valid. It would be interesting to check this further.

⁴⁴In fact, as shown in [40] the map between the VMS and 3d gravity works term by term also for partition functions, and with this also for their Laplace transforms (the resolvent analogue). In this sense the discussion in subsection 5.1 applies here too.

⁴⁵Of course one has to also include ZZ-branes in the full 'gravity' transseries with their own new transseries parameters. Here for brevity we omit them as the inclusion is straightforward. See also [57].

⁴⁶Perhaps also the approach in the recent work [64] can shed some light on this matter.

⁴⁷In the scaling limit to JT gravity the VMS energy E scales with b^2 . This follows from the scaling for P in [36].

$$R^{\text{FZZT}^+}(E) \simeq -\frac{i}{4E} \left(1 + g_s \frac{17 - 2\pi^2 E}{12(-E)^{3/2}} - g_s^2 \frac{1225 - 644\pi^2 E + 148\pi^4 E^2}{288E^3} + \dots \right) e^{+\frac{\tilde{A}(E)}{g_s}}, \quad (5.37)$$

where the FZZT action reads [43]

$$\tilde{A}(E) = \frac{1}{4\pi^3} \left(\sin \left(2\pi\sqrt{-E} \right) - 2\pi\sqrt{-E} \cos \left(2\pi\sqrt{-E} \right) \right). \quad (5.38)$$

After anti-Stokes transition – and as given in formula (5.17) – this action becomes

$$\tilde{\tilde{A}}(E) = \frac{1}{4\pi^3} \left(\sinh \left(2\pi\sqrt{E} \right) - 2\pi\sqrt{E} \cos \left(2\pi\sqrt{E} \right) \right). \quad (5.39)$$

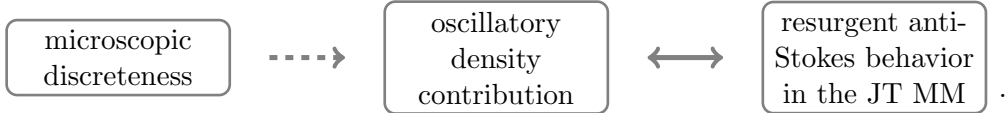
With this we can spell out the non-perturbative FZZT corrections to the JT gravity density to higher g_s orders. We then find

$$\langle \varrho_{\text{JT}}(E) \rangle \simeq -\frac{1}{8\pi E} \left(1 - g_s \frac{17 - 2\pi^2 E}{12(-E)^{3/2}} - g_s^2 \frac{1225 - 644\pi^2 E + 148\pi^4 E^2}{288E^3} + \dots \right) e^{-\frac{\tilde{A}(E)}{g_s}}, \quad (5.40)$$

for the density on the negative real line ($E < 0$). Taking into account the extra square root branch cuts in (5.36) and (5.37) we find on the positive real line

$$\begin{aligned} \langle \varrho_{\text{JT}}(E) \rangle &\simeq \sum_{g=0}^{\infty} g_s^{2g-1} \varrho_g(E) - \\ &- \frac{1}{4\pi E} \left(1 + g_s \cdot 0 + g_s^2 \frac{1225 - 644\pi^2 E + 148\pi^4 E^2}{288E^3} + \mathcal{O}(g_s^3) \right) \cos \left(\frac{\tilde{\tilde{A}}(E)}{g_s} \right) - \\ &- \left(g_s \frac{17 - 2\pi^2 E}{48\pi(-E)^{5/2}} + \mathcal{O}(g_s^2) \right) \sin \left(\frac{\tilde{\tilde{A}}(E)}{g_s} \right) + \\ &+ (\tau_2 + \tau_1) \frac{i}{4\pi E} \left(1 + g_s \cdot 0 + g_s^2 \frac{1225 - 644\pi^2 E + 148\pi^4 E^2}{288E^3} + \mathcal{O}(g_s^3) \right) \sin \left(\frac{\tilde{\tilde{A}}(E)}{g_s} \right) + \\ &- (\tau_2 - \tau_1) \left(g_s \frac{17 - 2\pi^2 E}{48\pi(-E)^{5/2}} + \mathcal{O}(g_s^2) \right) \sin \left(\frac{\tilde{\tilde{A}}(E)}{g_s} \right), \quad E > 0. \end{aligned} \quad (5.41)$$

We can conclude that the structure of formula (5.3) gets slightly more intricate when adding higher g_s orders. Nevertheless the main features stay the same: There is a universal oscillating piece dictated by Stokes constants and another also oscillating part that depends on the transseries parameters. To make contact with an actual function the transseries above still needs to be resummed. Last but not least we can connect the anti-Stokes behavior of the FZZT-branes with the idea that the oscillations in the eigenvalue density might originate from discreteness of microscopic hamiltonians drawn from the ensemble [60, 10, 61]. We can then make the connection



Given an ensemble description, the above construction constitutes a direct connection between the statistical properties of black holes and resurgent methods for FZZT-branes. This demonstrates that these methods can be used to study gravity via the matrix model approach.

Acknowledgments

It is a pleasure to thank Marcos Mariño, Ricardo Schiappa and Jasper Kager for a careful reading of the manuscript. We would furthermore like to thank Ricardo Schiappa for pointing us to the connection between the VMS and 3d gravity. Lastly we would like to thank Marcos Mariño, Ricardo Schiappa, Raghu Mahajan, Noam Tamarin, João Rodrigues and Jasper Kager for useful discussions, comments and/or correspondence. MS was partially supported by the Swiss National Science Foundation under grant number 185723 and grant number 200021_219267. This paper is partly a result of the ERC-SyG project, Recursive and Exact New Quantum Theory (ReNewQuantum) funded by the European Research Council (ERC) under the European Union's Horizon 2020 research and innovation programme, grant agreement 810573.

A Data for the Virasoro Minimal String

Here we present some of the data points used in the main text. It is produced with a slightly modified version of the MATHEMATICA file provided in [36]. Let us start by giving some coefficients for the free energy (2.1). We have

$$F_{V,2} = \frac{43c^3}{238878720} - \frac{559c^2}{79626240} + \frac{6691c}{79626240} - \frac{72007}{238878720}, \quad (\text{A.1})$$

$$F_{V,3} = \frac{176557c^6}{14794122225254400} - \frac{2295241c^5}{2465687037542400} + \frac{4089107c^4}{140896402145280} - \frac{340534753c^3}{739706111262720} + \frac{2740875239c^2}{704482010726400} - \frac{8112433381c}{493137407508480} + \frac{396807114421}{14794122225254400}, \quad (\text{A.2})$$

$$F_{V,4} = \frac{1959225867017c^9}{667926185350848999063552000} - \frac{25469936271221c^8}{74214020594538777673728000} + \frac{9203210865259c^7}{530100147103848411955200} - \frac{3953544371405837c^6}{7951502206557726179328000} + \frac{9392348683949221c^5}{1060200294207696823910400} - \frac{76863561439881203c^4}{757285924434069159936000} + \frac{41450007951172042679c^3}{55660515445904083255296000} - \frac{62278985594273187389c^2}{18553505148634694418432000} + \frac{24874755570604002257c}{2968560823781551106949120} - \frac{5843451389177575283669}{667926185350848999063552000}. \quad (\text{A.3})$$

Furthermore we used the resolvent (2.45), where the coefficients grow quickly in size. Let us nevertheless list one here

$$R_{g,2}^{(b)}(-z^2) = \frac{\pi^8}{20384317440\sqrt{2}\pi^9 z^{11}} \left((c-26)c(145(c-26)c + 40722) + 2782913 \right) z^8 + 12\pi^6(c-13)(169(c-26)c + 23713)z^6 + 180\pi^4(139(c-26)c + 22099)z^4 + 219240\pi^2(c-13)z^2 + 1020600. \quad (\text{A.4})$$

We have computed them up to order 14. And finally the genus 1 coefficient for a partition function with two boundaries that we used for the 3d gravity discussion reads

$$Z_{1,2}(\beta_1, \beta_2) = \quad (\text{A.5})$$

$$= \frac{\sqrt{\beta_1}\sqrt{\beta_2} (24\beta_1^2 + 24\beta_2^2 + \pi^4 (c^2 - 26c + 153)) + 8\beta_1 (3\beta_2 + \pi^2(c - 13)) + 8\pi^2\beta_2(c - 13)}{73728\pi^7}.$$

We have computed the series $Z_{g,2}$ up to $g = 12$.

References

- [1] J. Polchinski, *Combinatorics of Boundaries in String Theory*, Phys. Rev. **D50** (1994) R6041, arXiv:[hep-th/9407031](#).
- [2] J. Polchinski, *Dirichlet Branes and Ramond-Ramond charges*, Phys. Rev. Lett. **75** (1995) 4724, arXiv:[hep-th/9510017](#).
- [3] F. David, *Phases of the Large N Matrix Model and Nonperturbative Effects in 2D Gravity*, Nucl. Phys. **B348** (1991) 507, DOI:[10.1016/0550-3213\(91\)90202-9](#).
- [4] F. David, *Nonperturbative Effects in Matrix Models and Vacua of Two-Dimensional Gravity*, Phys. Lett. **B302** (1993) 403, arXiv:[hep-th/9212106](#).
- [5] S.Yu. Alexandrov, V.A. Kazakov, D. Kutasov, *Nonperturbative Effects in Matrix Models and D-Branes*, JHEP **09** (2003) 057, arXiv:[hep-th/0306177](#).
- [6] M. Mariño, R. Schiappa, M. Weiss, *Nonperturbative Effects and the Large-Order Behavior of Matrix Models and Topological Strings*, Commun. Number Theor. Phys. **2** (2008) 349, arXiv:[0711.1954](#)[hep-th].
- [7] M. Mariño, R. Schiappa, M. Weiss, *Multi-Instantons and Multi-Cuts*, J. Math. Phys. **50** (2009) 052301, arXiv:[0809.2619](#)[hep-th].
- [8] M. Mariño, *Nonperturbative Effects and Nonperturbative Definitions in Matrix Models and Topological Strings*, JHEP **0812** (2008) 114, arXiv:[0805.3033](#)[hep-th].
- [9] A. Klemm, M. Mariño, M. Rauch, *Direct Integration and Non-Perturbative Effects in Matrix Models*, JHEP **1010** (2010) 004, arXiv:[1002.3846](#)[hep-th].
- [10] P. Saad, S.H. Shenker, D. Stanford, *JT Gravity as a Matrix Integral*, arXiv:[1903.11115](#)[hep-th].
- [11] P. Gregori, R. Schiappa, *From Minimal Strings towards Jackiw–Teitelboim Gravity: On their Resurgence, Resonance, and Black Holes*, arXiv:[2108.11409](#)[hep-th].
- [12] R. Mahajan, D. Stanford and C. Yan, JHEP **07** (2022), 132 doi:10.1007/JHEP07(2022)132 arXiv:[2107.01172](#)[hep-th].
- [13] D.S. Eniceicu, R. Mahajan, C. Murdia, A. Sen, *Normalization of ZZ Instanton Amplitudes in Minimal String Theory*, JHEP **07** (2022) 139, arXiv:[2202.03448](#)[hep-th].
- [14] D.S. Eniceicu, R. Mahajan, C. Murdia, A. Sen, *Multi-Instantons in Minimal String Theory and in Matrix Integrals*, JHEP **10** (2022) 065, arXiv:[2206.13531](#)[hep-th].
- [15] M. Mariño, R. Schiappa, M. Schwick, *New Instantons for Matrix Models*, arXiv:[2210.13479](#)[hep-th].
- [16] D. S. Eniceicu, R. Mahajan, P. Maity, C. Murdia and A. Sen, JHEP **12** (2022), 151 doi:10.1007/JHEP12(2022)151 arXiv:[2210.11473](#)[hep-th].
- [17] D.S. Eniceicu, *Comments on the Giant-Graviton Expansion of the Superconformal Index*, arXiv:[2302.04887](#)[hep-th].
- [18] R. Schiappa, M. Schwick, N. Tamarin, *All the D-Branes of Resurgence*, arXiv:[2301.05214](#)[hep-th].
- [19] V. Chakrabhavi, D.S. Eniceicu, R. Mahajan, C. Murdia, *Normalization of ZZ Instanton Amplitudes in Type 0B Minimal Superstring Theory*, JHEP **09** (2024) 114, arXiv:[2406.16867](#)[hep-th].
- [20] S. Alexandrov, R. Mahajan and A. Sen, JHEP **01** (2024), 141 doi:10.1007/JHEP01(2024)141 arXiv:[2311.04969](#)[hep-th].
- [21] D.S. Eniceicu, R. Mahajan, C. Murdia, *Complex Eigenvalue Instantons and the Fredholm Determinant Expansion in the Gross–Witten–Wadia Model*, JHEP **01** (2024) 129, arXiv:[2308.06320](#)[hep-th].

- [22] D.S. Eniceicu, C. Murdia, A. Torchylo, *The Complete Non-Perturbative Partition Function of Minimal Superstring Theory and JT Supergravity*, JHEP **06** (2025) 178, [arXiv:2412.08698](#) [hep-th].
- [23] A.B. Zamolodchikov, Al.B. Zamolodchikov, *Liouville Field Theory on a Pseudosphere*, in “6th Workshop on Supersymmetries and Quantum Symmetries” (2001) 280, [arXiv:hep-th/0101152](#).
- [24] V. Fateev, A.B. Zamolodchikov, Al.B. Zamolodchikov, *Boundary Liouville Field Theory I: Boundary State and Boundary Two Point Function*, [arXiv:hep-th/0001012](#).
- [25] J. Teschner, *Remarks on Liouville Theory with Boundary*, in “4th Annual European TMR Conference on Integrability Nonperturbative Effects and Symmetry in Quantum Field Theory” (2000) 041, [arXiv:hep-th/0009138](#).
- [26] S. Garoufalidis, A. Its, A. Kapaev, M. Mariño, *Asymptotics of the Instantons of Painlevé I*, Int. Math. Res. Notices **2012** (2012) 561, [arXiv:1002.3634](#) [math.CA].
- [27] I. Aniceto, R. Schiappa, M. Vonk, *The Resurgence of Instantons in String Theory*, Commun. Number Theor. Phys. **6** (2012) 339, [arXiv:1106.5922](#) [hep-th].
- [28] S. Baldino, R. Schiappa, M. Schwick, R. Vega, *Resurgent Stokes Data for Painlevé Equations and Two-Dimensional Quantum (Super) Gravity*, Commun. Number Theor. Phys. **17** (2023) 385, [arXiv:2203.13726](#) [hep-th].
- [29] R. Schiappa, R. Vaz, *The Resurgence of Instantons: Multi-Cut Stokes Phases and the Painlevé II Equation*, Commun. Math. Phys. **330** (2014) 655, [arXiv:1302.5138](#) [hep-th].
- [30] R. Vega, *Parametric Resurgences of the Second Painlevé Equation and Minimal Superstrings*, [arXiv:2311.03103](#) [hep-th].
- [31] J. Écalle, *Les Fonctions Résurgentes*, Publications Mathématiques d’Orsay **81-05** (1981), **81-06** (1981), **85-05** (1985).
- [32] S.H. Shenker, *The Strength of Nonperturbative Effects in String Theory*, in “The Large N Expansion in Quantum Field Theory and Statistical Physics” (1990) 809, DOI:[10.1142/9789814365802_0057](#).
- [33] M. Mariño, *Lectures on Nonperturbative Effects in Large N Gauge Theories, Matrix Models and Strings*, Fortsch. Phys. **62** (2014) 455, [arXiv:1206.6272](#) [hep-th].
- [34] D. Sauzin, *Introduction to 1-Summability and Resurgence*, in “Divergent Series, Summability and Resurgence I: Monodromy and Resurgence”, Lec. Notes Math. **2153** (2016), [arXiv:1405.0356](#) [math.DS].
- [35] I. Aniceto, G. Başar, R. Schiappa, *A Primer on Resurgent Transseries and Their Asymptotics*, Phys. Rept. **809** (2019) 1, [arXiv:1802.10441](#) [hep-th].
- [36] S. Collier, L. Eberhardt, B. Mühlmann, V. Rodriguez, *The Virasoro Minimal String*, SciPost Phys. **16** (2024) no.2, 057 doi:10.21468/SciPostPhys.16.2.057 [arXiv:hep-th/2309.10846](#).
- [37] J. Kager, J. Rodrigues, R. Schiappa, M. Schwick, N. Tamarin, *Exact Solutions to Matrix Models and String Theories: The Local Construction*, [arXiv:2602.15101](#) [hep-th].
- [38] B. Eynard, M. Mariño, *A Holomorphic and Background Independent Partition Function for Matrix Models and Topological Strings*, J. Geom. Phys. **61** (2011) 1181, [arXiv:0810.4273](#) [hep-th].
- [39] D. L. Jafferis, L. Rozenberg and G. Wong, *3d gravity as a random ensemble*, JHEP **02** (2025), 208 doi:10.1007/JHEP02(2025)208 [arXiv:2407.02649](#) [hep-th].
- [40] D. L. Jafferis, L. Rozenberg, D. Sarkar and D. Wang, *On random matrix statistics of 3d gravity*, [arXiv:2512.05045](#) [hep-th] (2025), <https://arxiv.org/abs/2512.05045>.
- [41] C. Teitelboim, *Gravitation and Hamiltonian Structure in Two Space-Time Dimensions*, Phys. Lett. **126B** (1983) 41, DOI:[10.1016/0370-2693\(83\)90012-6](#).

- [42] R. Jackiw, *Lower Dimensional Gravity*, Nucl. Phys. **B252** (1985) 343, DOI:[10.1016/0550-3213\(85\)90448-1](https://doi.org/10.1016/0550-3213(85)90448-1).
- [43] B. Eynard, E. Garcia-Failde, P. Gregori, D. Lewański, R. Schiappa, *Resurgent Asymptotics of Jackiw–Teitelboim Gravity and the Nonperturbative Topological Recursion*, arXiv:[2305.16940](https://arxiv.org/abs/2305.16940) [hep-th].
- [44] B. Eynard, N. Orantin, *Invariants of Algebraic Curves and Topological Expansion*, Commun. Num. Theor. Phys. **1** (2007) 347, arXiv:[math-ph/0702045](https://arxiv.org/abs/math-ph/0702045).
- [45] T. Okuda, T. Takayanagi, *Ghost D-Branes*, JHEP **03** (2006) 062, arXiv:[hep-th/0601024](https://arxiv.org/abs/hep-th/0601024).
- [46] D. Gaiotto, G. W. Moore and A. Neitzke, *Wall-crossing, Hitchin systems, and the WKB approximation*, Adv. Math. **234** (2013), 239-403 doi:10.1016/j.aim.2012.09.027 arXiv:[0907.3987](https://arxiv.org/abs/0907.3987) [hep-th].
- [47] M. Mariño, M. Schwick, *Large N instantons, BPS states, and the replica limit*, arXiv:[2403.14462](https://arxiv.org/abs/2403.14462) [hep-th] (2024).
- [48] R. Schiappa, M. Schwick, *Exact Solutions to Matrix Models and String Theories: Background Independence of the Large N Expansions*, (2026).
- [49] N. Seiberg and D. Shih, *Branes, rings and matrix models in minimal (super)string theory*, JHEP **02** (2004), 021 doi:10.1088/1126-6708/2004/02/021 arXiv:[hep-th/0312170](https://arxiv.org/abs/hep-th/0312170) [hep-th].
- [50] N. Seiberg and D. Shih, *Minimal string theory*, Comptes Rendus Physique **6** (2005), 165-174 doi:10.1016/j.crhy.2004.12.007 arXiv:[hep-th/0409306](https://arxiv.org/abs/hep-th/0409306) [hep-th].
- [51] G. Borot, B. Eynard and A. Giacchetto, *The factorial growth of topological recursion*, Lett. Math. Phys. **115**, 62 (2025), <https://doi.org/10.1007/s11005-025-01950-z>.
- [52] A. Grassi, Y. Hatsuda and M. Marino, *Topological Strings from Quantum Mechanics*, Annales Henri Poincaré **17** (2016) no.11, 3177-3235 doi:10.1007/s00023-016-0479-4 arXiv:[1410.3382](https://arxiv.org/abs/1410.3382) [hep-th].
- [53] G. Bonelli, O. Lisovyy, K. Maruyoshi, A. Sciarappa, A. Tanzini, *On Painlevé/Gauge Theory Correspondence*, Lett. Math. Phys. **107** (2017) 2359, arXiv:[1612.06235](https://arxiv.org/abs/1612.06235) [hep-th].
- [54] G. Bonnet, F. David and B. Eynard, *Breakdown of universality in multicut matrix models*, J. Phys. A **33** (2000), 6739-6768 doi:10.1088/0305-4470/33/38/307 arXiv:[cond-mat/0003324](https://arxiv.org/abs/cond-mat/0003324) [cond-mat].
- [55] D. L. Jafferis, L. Rozenberg and D. Wang, *Open-closed 3d gravity as a random ensemble*, JHEP **2025**, 228 (2025), [https://doi.org/10.1007/JHEP10\(2025\)228](https://doi.org/10.1007/JHEP10(2025)228), arXiv:2506.19817 [hep-th].
- [56] K. Okuyama and K. Sakai, *JT gravity, KdV equations and macroscopic loop operators*, JHEP **01** (2020), 156 doi:10.1007/JHEP01(2020)156 arXiv:[1911.01659](https://arxiv.org/abs/1911.01659) [hep-th].
- [57] C. V. Johnson and J. Rodrigues, *Non-perturbative data for Weil-Petersson volumes and intersection numbers using ordinary differential equations*, arXiv:[2601.03351](https://arxiv.org/abs/2601.03351) [hep-th].
- [58] M. Marino, *Les Houches lectures on matrix models and topological strings*, arXiv:[hep-th/0410165](https://arxiv.org/abs/hep-th/0410165) [hep-th].
- [59] D. Berenstein, J. Rodrigues and V. A. Rodriguez, *Asymptotic bootstrap for unitary matrix integrals at complex coupling*, arXiv:[2602.18559](https://arxiv.org/abs/2602.18559) [hep-th].
- [60] P. Saad, S. H. Shenker and D. Stanford, *A semiclassical ramp in SYK and in gravity*, arXiv:[1806.06840](https://arxiv.org/abs/1806.06840) [hep-th].
- [61] D. Stanford and E. Witten, Adv. Theor. Math. Phys. **24** (2020) no.6, 1475-1680 doi:10.4310/ATMP.2020.v24.n6.a4 arXiv:[1907.03363](https://arxiv.org/abs/1907.03363) [hep-th].
- [62] J. Gu and M. Marino, *Exact multi-instantons in topological string theory*, SciPost Phys. **15** (2023) no.4, 179 doi:10.21468/SciPostPhys.15.4.179 arXiv:[2211.01403](https://arxiv.org/abs/2211.01403) [hep-th].

- [63] Q. Hao, *Exact WKB of solutions by Borel summation and open TBA*, [arXiv:2507.06922](#) [hep-th] (2025)
- [64] A. Belin, S. Collier, L. Eberhardt, D. Liska and B. Post, *A universal sum over topologies in 3d gravity*, [arXiv:2601.07906](#) [hep-th].